Thesis

Econophysics on Interactions of Markets

Yukihiro Aiba

Department of Physics, Graduate School of Science, University of Tokyo

December 2005

Acknowledgments

I would like to express my sincere gratitude to Professor Naomichi Hatano, for his guidance, useful discussions, and encouragements. Without his cordial support, this work has never been performed. I also would like to express my sincere gratitude to Dr. Hideki Takayasu for his guidance and fruitful discussions.

I am grateful to Prof. Hajime Takayama, Prof. Miki Wadati, Prof. Kazuyuki Aihara, Prof. Shinichi Sasa and Prof. Naoki Kawashima for their critical reading of the manuscript and useful comments. I would like to thank all members of Hatano Laboratory for stimulating discussions and encouragements. In particular, I would like to thank Mr. Tetsuro Murai, Ms. Junko Yamasaki, Mr. Masahiro Kawakami, Mr. Kouhei Oikawa, Mr. Kenji Kawamura, Dr. Manabu Machida, Dr. Shunji Tsuchiya, Dr. Akinori Nishino, Dr. Keita Sasada, Dr. Yuichi Nakamura, Mr. Masashi Fujinaga and Mr. Naoya Sato for stimulating discussions and their encouragements.

I acknowledge the financial support from University of Tokyo 21st Century COE Program "Quantum Extreme System and Their Symmetries."

Finally, I thank my family and all of my friends for their continual encouragement and support.

Contents

1 Introduction: What is Econophysics? 1
- 1.1 Economic systems as strongly correlated many-body systems . 1
- 1.2 Scaling properties of financial prices 2
- 1.3 Econophysics of wealth distributions 3
- 1.4 An example of modeling financial fluctuations using concepts of statistical physics 6
  - 1.4.1 Sznajd model 6
  - 1.4.2 Sato and Takayasu's dealer model 10
- 1.5 Summary 14
- 1.6 The contents of the thesis 18

2 Triangular Arbitrage as an Interaction among Foreign Exchange Rates 19
- 2.1 Introduction 19
- 2.2 Existence of triangular arbitrage opportunities 20
- 2.3 Feasibility of the triangular arbitrage transaction 21

3 A Macroscopic Model of Triangular Arbitrage Transaction 29
- 3.1 Macroscopic model of triangular arbitrage 29
  - 3.1.1 Basic time evolution 30
  - 3.1.2 Estimation of parameters 32
  - 3.1.3 Analytical approach 36
- 3.2 Negative auto-correlation of the foreign exchange rates in a short time scale 38
- 3.3 What makes the rate product converge 40

4 A Microscopic Model of Triangular Arbitrage Transaction 43
- 4.1 Introduction 43

4.2 Microscopic model of triangular arbitrage 44
4.2.1 Microscopic model of triangular arbitrage: interacting two systems of the ST model 44
4.3 The microscopic parameters and the macroscopic spring constant 48

5 Summary **55**

Chapter 1

Introduction: What is Econophysics?

1.1 Economic systems as strongly correlated many-body systems

Systems consisting of many interacting units such as strongly correlated many-body systems are of great interest of statistical physics. In such systems, exotic phenomena like phase transitions occur, but we cannot see them emerging if we look at each unit separately. Statistical physics treats the interacting units as a whole and thereby have successfully elucidated the mechanism of the phenomena.

Economic systems obviously consist of a large number of interacting units. Thus one may expect it possible that methods and concepts developed in the study of strongly correlated systems may yield new results in economics. In fact, some empirical laws are founded and models aiming to reproduce such phenomena are constructed, using the methods and the concepts developed in statistical physics.

Econophysics is a word used to describe work being done by physicists in which financial and economic systems are treated as complex systems [1, 2]. Many physicists have contributed to quantifying and modeling economic fluctuations in recent years.

The content of this chapter is in preparation for submission.

1.2 Scaling properties of financial prices

Mandelbrot, who is famous as the advocator of the concept of *fractal*, originally found a self-similar structure by analyzing the fluctuations of the cotton price in a commodity market [3]. Recently, Mantegna and Stanley [4, 5, 6, 7] found a scaling law in the fluctuations of a stock index. The stock index is a weighted average of the stock prices. Specifically, Mantegna and Stanley used a stock index called the S&P 500. They analyzed the price fluctuation of the S&P 500 as follows. Let $G(T)$ be the logarithm of the price change in a time step T [min]:

$$G(T) = \ln Y(t) - \ln Y(t-T), \tag{1.1}$$

where $Y(t)$ is the price at time t. The value G is often called 'return.' Mantegna and Stanley drew the histograms $P(G)$ for the time steps T =1, 3, 10, 32, 100, 316, 1000 [min] (Fig. 1.1). The shape of the histogram of course depends on T; it spreads as T increases. However, the histograms for various values of T collapsed onto one curve by scaling

$$\tilde{G} \equiv \frac{G}{T^{1/\beta}} \tag{1.2}$$

and

$$\tilde{P}(\tilde{G}) \equiv \frac{P(\tilde{G})}{T^{-1/\beta}}, \tag{1.3}$$

where $\beta = 1.4$. This fact means that the price fluctuations have a self-similar structure often found in critical phenomena in physical systems.

Gopikrishnan *et al.* [8, 9] later analyzed a database documenting each and every trade in the three major US stock markets, the New York Stock Exchange (NYSE), the American Stock Exchange (AMEX), and the National Association of Securities Dealers Automated Quotation (NASDAQ) for the entire two-year period. They thereby extracted a sample of approximately 4 million data points, which is much larger than the 500 thousand data points analyzed by Mantegna and Stanley, and the 2000 data points studied by Mandelbrot. Gopikrishnan *et al.* found an asymptotic power-law behavior with an exponent $\beta \simeq 3$ for the cumulative distribution (Fig. 1.2). They refer to this phenomenon as an '*inverse cubic law*' [10].

The power-law behavior was also found in the foreign exchange markets [11, 12, 13]. These results motivated many physicists to analyze financial fluctuations and to find '*universality*' in the economic system in recent years.

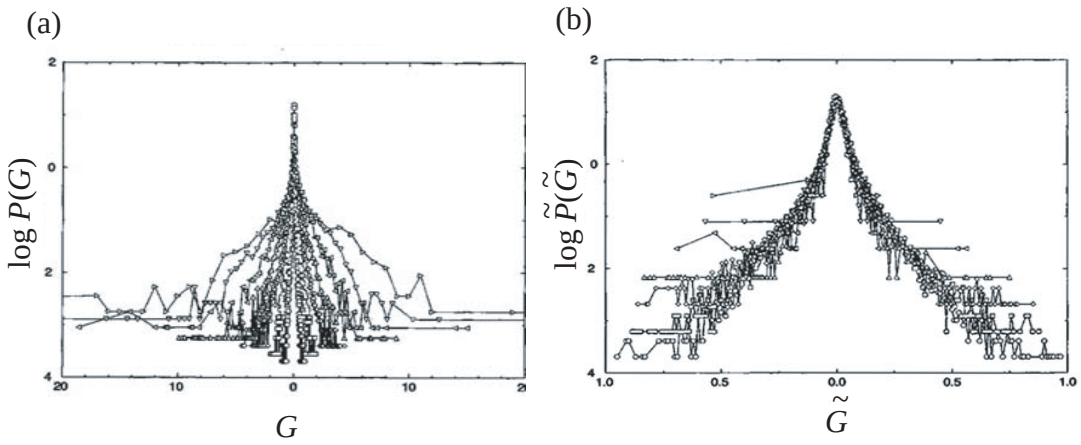

Figure 1.1: (a) The probability density functions of price changes measured at different time horizons T=1, 3, 10, 32, 100, 316, 1000 minutes. The distributions spread with increasing T. (b) The same data as in (a), but plotted in scaled units. The distributions collapse well onto the distribution for T=1 [min]. Both graphs are adapted from [4].

1.3 Econophysics of wealth distributions

Another important topic in econophysics is a power-law behavior of wealth distributions [14]. Here, the 'wealth' means the income of individuals, the size of business firms or the GDP of countries.

The fact that wealth distributions have power-law tails has been recognized for over 100 years. Pareto [15] investigated the statistics of the wealth of individuals by modeling them as a scale-invariant distribution

$$f(x) \sim x^{-\gamma}, \tag{1.4}$$

where $f(x)$ denotes the number of people having income equal to or greater than x, and γ is an exponent that Pareto estimated to be 1.5. Nowadays, many works have analyzed the data of personal income and modeled them [16]–[20].

The size distributions of business firms also obey the power law. Okuyama *et al.* [21] analyzed the income of business firms in Japan and Italy. Figure 1.3 is a logarithmic plot of the distributions of the income of Japanese and Italian companies. The data for the Japanese firms can be approximated by

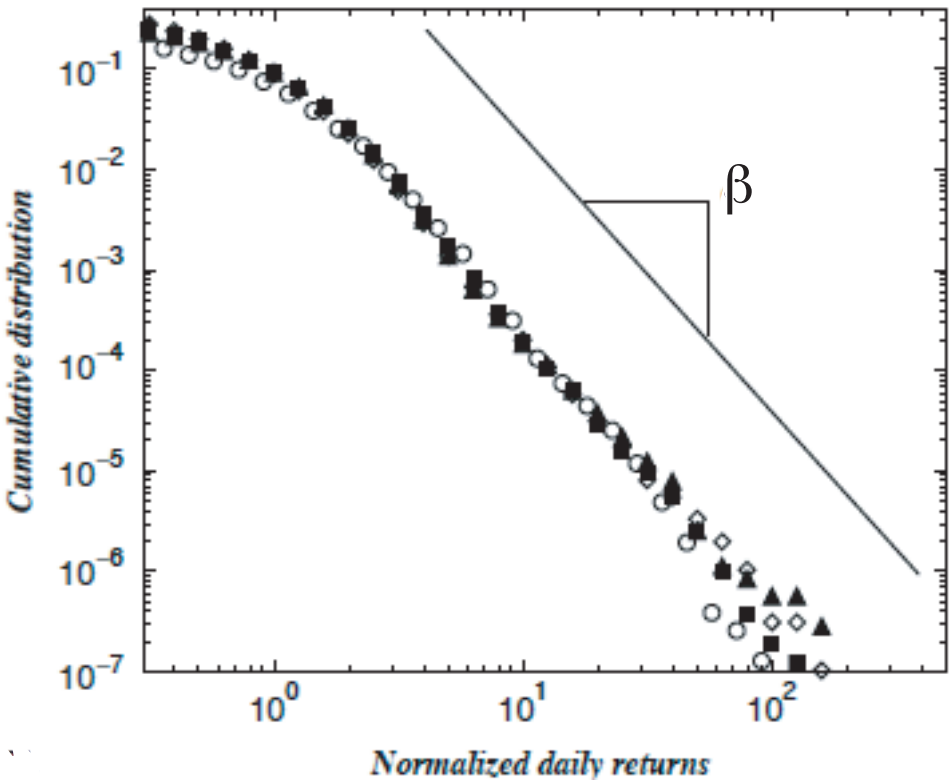

Figure 1.2: The cumulative distribution of normalized daily price changes. The price change is often called 'return.' This graph is adapted from [10].

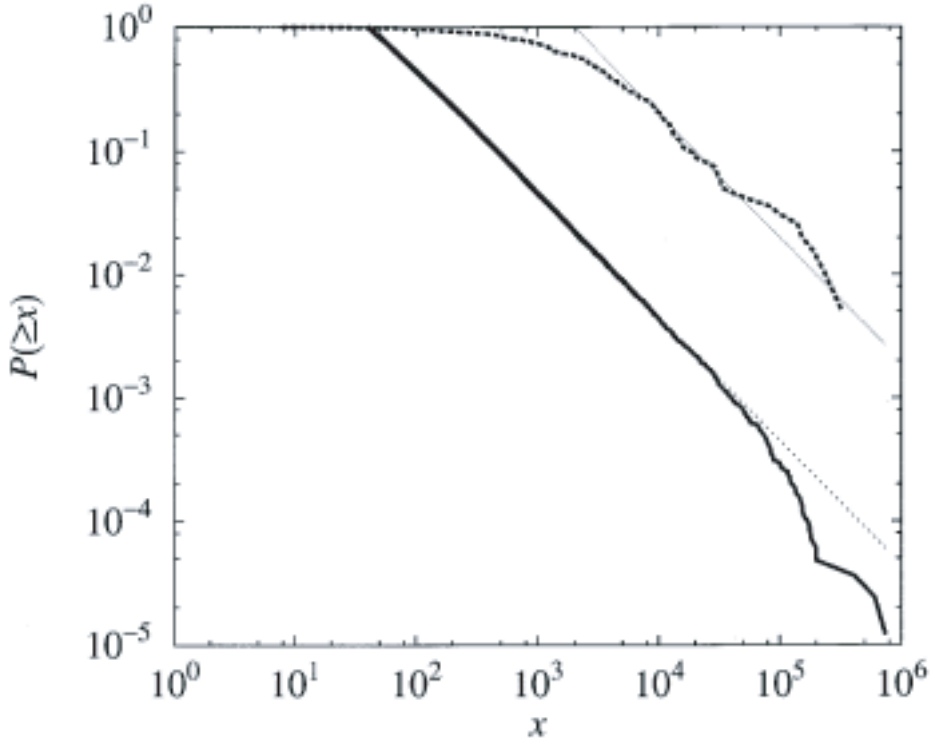

Figure 1.3: The cumulative distribution of the income of Japanese companies (the bold line with x a million yen) and Italian firms (the dashed line with x a hundred thousand lira). The two straight lines show the power law with the exponent -1, namely Zipf's law. This graph is adapted from [21].

a straight line with slope -1 in the range of income less than 10^5; this means that the distribution follows a power law with an exponent very close to -1, namely Zipf's law. The data for the Italian firms are roughly on a straight line with the same slope -1, but the Italian data deviate from the straight line in comparison to the Japanese data. Okuyama *et al.* concluded that this was because of the lack of data of smaller companies.

Furthermore, M.H.R. Stanley *et al.* [22, 23] calculated histograms of how the firm size changes from one year to the next. They made 15 histograms for each of 15 bins of the firm size. The largest firms have very narrow distributions of growth rates. This means that the percentage of the size

change from year to year for the largest firms cannot be so great. A tiny firm, on the other hand, can radically increase or decrease in size from year to year. These 15 histograms thus have widths that depend on the firm size. The width showed a power law of the firm size with an exponent $\lambda \simeq 1/6$ over 8 orders of magnitude, from the tiniest firm to the largest firm [22, 23]. The growth rate therefore can be normalized and the data collapse on a single curve.

This scaling property can be extended to the growth rate of countries by analyzing the GDP. Lee *et al.* [24] found that the histograms of the country size in the GDP behave the same way as the histograms of the firm size. They analyzed the annual growth rate $R \equiv \ln[g(t+1)/g(t)]$, where $g(t)$ is the GDP of a country in the year t. They found that, for all countries and years, the probability density of R is consistent with an exponential decay for a certain range of $|R|$ (see Fig. 1.4(a)). In order to investigate the dependence of the growth rate on the initial value of the GDP, they divided the countries into groups according to their GDPs. The empirical conditional probability density of R for countries is also consistent with an exponential form in a range (see Fig. 1.4(b)). They found that the conditional probability density of R for countries can be scaled by its standard deviation. The results are in quantitative agreement with findings for the growth of firms [22, 23, 25, 26] (see Fig. 1.5).

1.4 An example of modeling financial fluctuations using concepts of statistical physics

There are many models aiming to reproduce the price fluctuations in the financial market (for example, [27]–[32]). Here we first review the Sznajd model of price formation proposed by Sznajd-Weron and Weron [32]. Next, we review Sato and Takayasu's dealer model [29]. These models well reproduce the power-law behavior of the price fluctuation by quite different approaches.

1.4.1 Sznajd model

The time evolution of the Sznajd model are as follows. Prepare an Ising chain consisting of N spins S_i with a periodic boundary condition. Regard the spins as traders in a financial market. The directions of the spins represent traders'

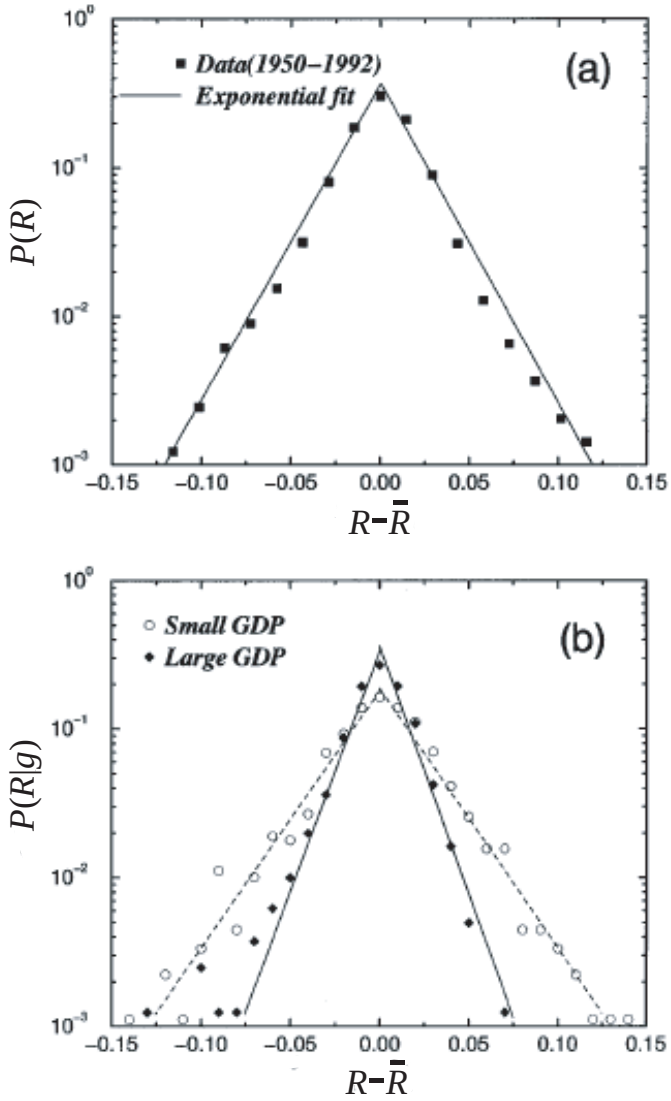

Figure 1.4: (a) The probability density function of the annual growth rate. Shown are the average annual growth rates for the entire period 1950–1992 together with an exponential fit. (b) The probability density function of the annual growth rate for two subgroups with different ranges of g, where g denotes the GDP detrended by the average yearly growth rate. The entire database was divided into three groups: $6.9\times10^7 \leq g < 2.4\times10^9$, $2.4\times10^9 \leq g < 2.2\times10^{10}$, and $2.2\times10^{10} \leq g < 7.6\times10^{11}$, and the figure shows the distributions for the groups with the smallest and the largest GDPs. Lee *et al.* considered only three subgroups in order to have enough events in each bin for the determination of the distribution. This graph is adapted from [24].

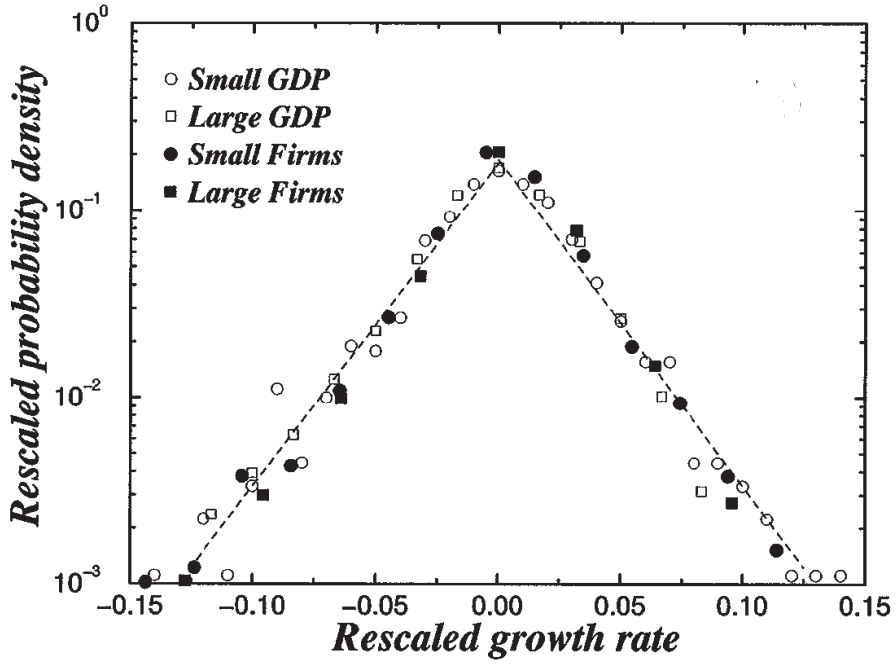

Figure 1.5: The conditional probability density of the annual growth rates of countries and firms. The data are rescaled by their standard deviations. All data collapse onto a single curve, showing that the distributions indeed have the same functional form. This graph is adapted from [24].

actions: if the ith spin is up, the ith trader wants to buy; if the ith spin is down, the ith trader wants to sell.

We now define the rule of opinion formation. Select a pair of consecutive traders S_i and S_{i+1} at random. If $S_iS_{i+1} = 1$, then make the directions of S_{i-1} and S_{i+2} the direction of $S_i (= S_{i+1})$. If $S_iS_{i+1} = -1$, then change the directions of S_{i-1} and S_{i+2} to ± 1 at random. Let the magnetization

$$m(t) = \frac{1}{N} \sum_{i=1}^{N} S_i(t) \tag{1.5}$$

be the price of the market, which is the normalized difference between demand and supply.

Obviously, the above model has two stable states, all spins up and all spins down. They are, however, not the states that we want to reproduce. In order to avoid this problem, let one of the N traders be a fundamentalist. The fundamentalist changes his/her direction depending on the price m. The fundamentalist buys, or takes the value 1 at time t with probability $|m(t)|$ if $m(t) < 0$ and sells, or takes the value -1 with probability $m(t)$ if $m(t) > 0$. This rule means that if the system becomes close to the stable state 'all up,' the fundamentalist will place a sell order, take the value -1 almost certainly and hence the system will start to reverse. When the price $m(t)$ is close to the other stable state 'all down,' on the other hand, the fundamentalist will place a buy order, take the value 1, and the price will start to grow. Thus the ferromagnetic states are made unstable states.

The dynamics of the price $m(t)$ simulated by the Sznajd model is shown in Fig. 1.6 together with the USD/DEM exchange rate. The returns $r(t) \equiv m(t) - m(t-1)$ are compared to the USD/DEM exchange rate in the top panels of Fig. 1.7 and the normal probability plot of $r(t)$ are compared to the USD/DEM returns in the bottom panels of Fig. 1.7. Sznajd-Weron *et al.* concluded that this simple model is a good first approximation of a number of real financial markets, because the results show good agreement with the actual market data.

This model is very simple at first sight; there is no connection between an Ising-like spin system and a financial market. Nonetheless, the model well reproduces the statistics of the price change in foreign exchange markets including the fat-tail behavior of the fluctuations. It is interesting that two systems having no connection at first sight behave similarly.

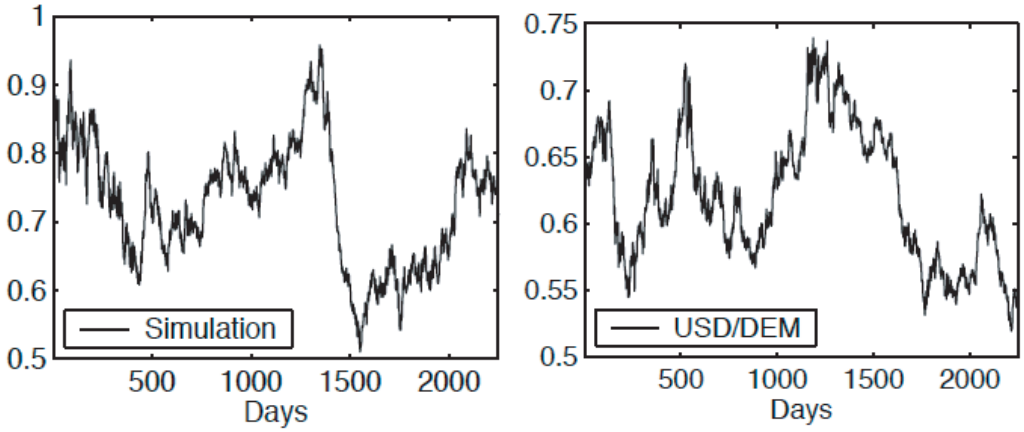

Figure 1.6: A typical fluctuation of the simulated price process $m(t)$ on the left with the USD/DEM exchange rate on the right. In the simulation, eight simulation steps are regarded as one day. This graph is adapted from [32].

1.4.2 Sato and Takayasu's dealer model

We next review Sato and Takayasu's dealer model (the ST model) briefly [29] (Fig. 1.8). The ST model also reproduces the power-law behavior of the price fluctuations. The basic assumption of the ST model is that dealers want to buy stocks or currencies at a lower price and to sell them at a higher price. There are N dealers; the ith dealer has bidding prices to buy, $B_i(t)$, and to sell, $S_i(t)$, at time t. We assume that the difference between the buying price and the selling price is a constant $\Lambda \equiv S_i(t) - B_i(t) > 0$ for all i, in order to simplify the model.

The model assumes that a trade takes place between the dealer who proposes the maximum buying price and the one who proposes the minimum selling price. A transaction thus takes place when the condition

$$\max\{B_i(t)\} \geq \min\{S_i(t)\} \tag{1.6}$$

or

$$\max\{B_i(t)\} - \min\{B_i(t)\} \geq \Lambda \tag{1.7}$$

is satisfied, where $\max\{\cdot\}$ and $\min\{\cdot\}$, respectively, denote the maximum and the minimum values in the set of the dealers' buying threshold $\{B_i(t)\}$.

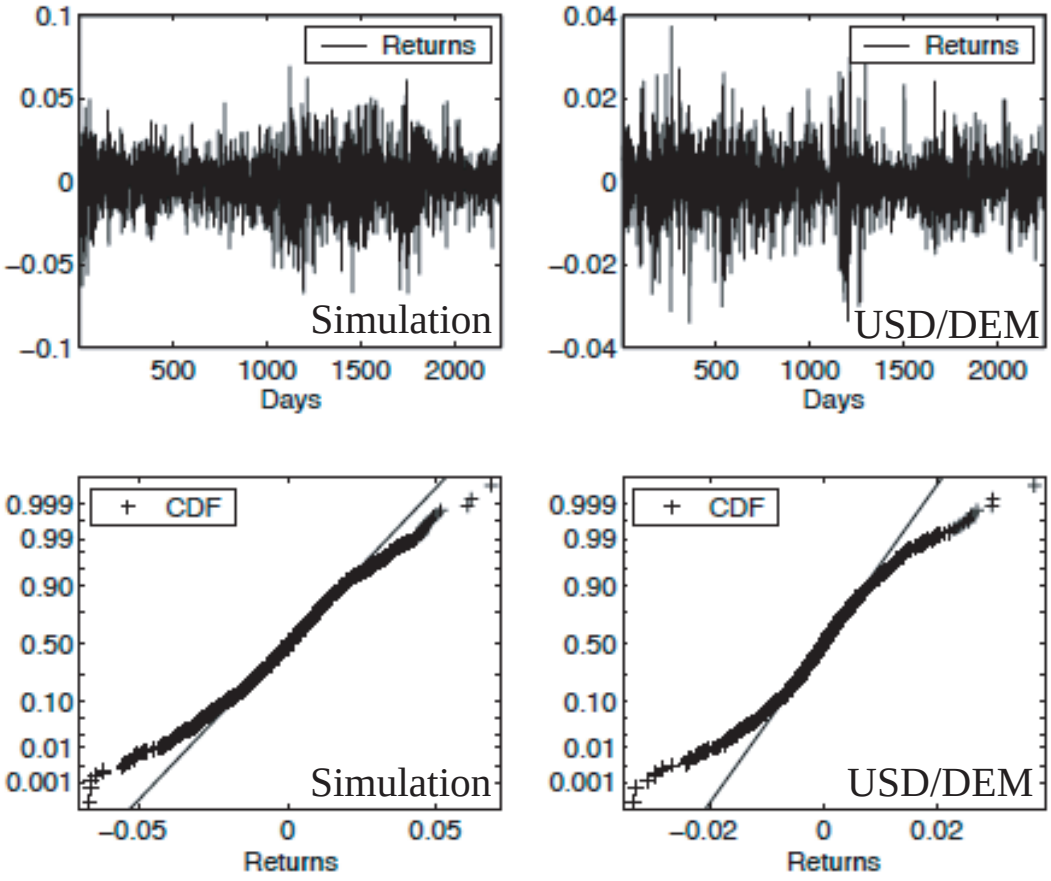

Figure 1.7: The returns $r(t)$ of the simulated price process $m(t)$ and daily returns of the USD/DEM exchange rate during the last decade, respectively (the top panels). The normal probability plots of $r(t)$ and USD/DEM returns, respectively, clearly show fat tails of the price-return distributions (the bottom panels). This graph is adapted from [32].

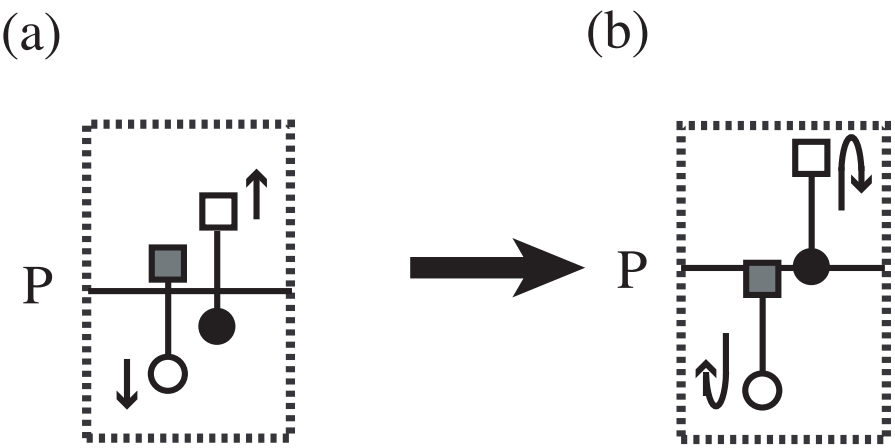

Figure 1.8: A schematic image of a transaction of the ST model. Only the best bidders are illustrated, in order to simplify the image. The circles denote the dealers' bidding price to buy and the squares denote the dealers' bidding price to sell. The filled circles denote the best bidding price to buy, $\max\{B_i\}$, and the grey circles denote the best bidding price to sell, $\min\{B_i\}+\Lambda$. In (a), the condition (1.7) is not satisfied, and the dealers, following Eq. (1.9), change their relative positions by a_i. Note that the term $c\Delta P$ does not depend on i; hence it does not change the relative positions of dealers but change the whole dealers' positions. In (b), the best bidders satisfy the condition (1.7). The price P is renewed according to Eq. (1.8), and the buyer and the seller, respectively, become a seller and a buyer according to Eq. (1.10).

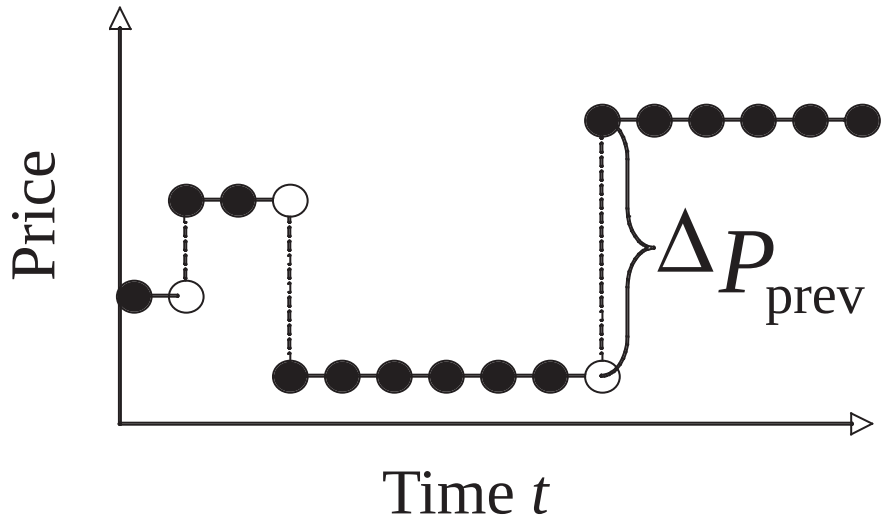

Figure 1.9: A schematic image of the price difference ΔP. The price difference ΔP is defined as the difference between the present price and the price at the time when the previous trade was done, and it maintains its value until the next trade happens.

The market price $P(t)$ is defined by the mean value of $\max\{B_i\}$ and $\min\{S_i\}$ when the trade takes place. The price $P(t)$ maintains its previous value when the condition (1.7) is not satisfied:

$$P(t) = \begin{cases} (\max\{B_i(t)\} + \min\{S_i(t)\})/2, & \text{if the condition (1.7) is satisfied,} \\ P(t-1), & \text{otherwise.} \end{cases} \tag{1.8}$$

The dealers change their prices in a unit time by the following deterministic rule:

$$B_i(t+1) = B_i(t) + a_i(t) + c\Delta P(t), \tag{1.9}$$

where $a_i(t)$ denotes the ith dealer's characteristic movement in the price at time t, $\Delta P(t)$ is the difference between the price at time t and the price at the time when the previous trade was done (see Fig. 1.9), and $c(>0)$ is a constant which specifies dealers' response to the market price change, and is common to all of the dealers in the market. The absolute value of a dealer's characteristic movement $a_i(t)$ is given by a uniform random number in the

range $[0, \alpha)$ and is fixed throughout the time. The sign of a_i is positive when the ith dealer is a buyer and is negative when the dealer is a seller. The buyer (seller) dealers move their prices up (down) until the condition (1.7) is satisfied. Once the transaction takes place, the buyer of the transaction becomes a seller and the seller of the transaction becomes a buyer; in other words, the buyer dealer changes the sign of a_i from positive to negative and the seller dealer changes it from negative to positive:

$$a_i(t+1) = \begin{cases} -a_i(t) & \text{for the buyer and the seller,} \\ a_i(t) & \text{for other dealers.} \end{cases} \tag{1.10}$$

The initial values of $\{B_i\}$ are given by uniform random numbers in the range $(-\Lambda, \Lambda)$. We thus simulate this model specifying the following four parameters: the number of dealers, N; the spread between the buying price and the selling price, Λ; the dealers' response to the market price change, c; and the average of dealers' characteristic movements in a unit time, α.

The ST model well reproduces the power-law behavior of the price change when the dealers' response to the market change $c > c^*$, where c^* is a critical value to the power-law behavior (Figs. 1.10 and 1.11). The critical point depends on the other parameters; *e.g.* $c^* \simeq 0.25$ for $N = 100$, $\Lambda = 1.0$ and $\alpha = 0.01$ [29]. For $c < c^*$, the probability distribution of the price change ΔP can be approximated by a hybrid distribution in the tails of $|\Delta P|$. For $c > c^*$ the probability distribution is approximated by a power law. As c increases, the distribution has longer tails and the exponent of the power-law distribution is estimated to be smaller. For c greater than 0.45, the price fluctuation is very unstable and diverges quickly; that is, one cannot observe any steady distributions. The probability distribution looks similar to the distribution of price changes for real stock markets reported by Mantegna and Stanley [4] in the case $c \simeq 0.3$ except the tail parts for very large $|\Delta P|$.

1.5 Summary

Economic systems consist of a large number of interacting units and exhibit various scaling properties. The fact has physicists anticipate the existence of a connection between the fluctuations in economic systems and critical phenomena in the physical systems. The methods and the concepts developed in statistical physics have been used to reproduce the financial fluctuations.

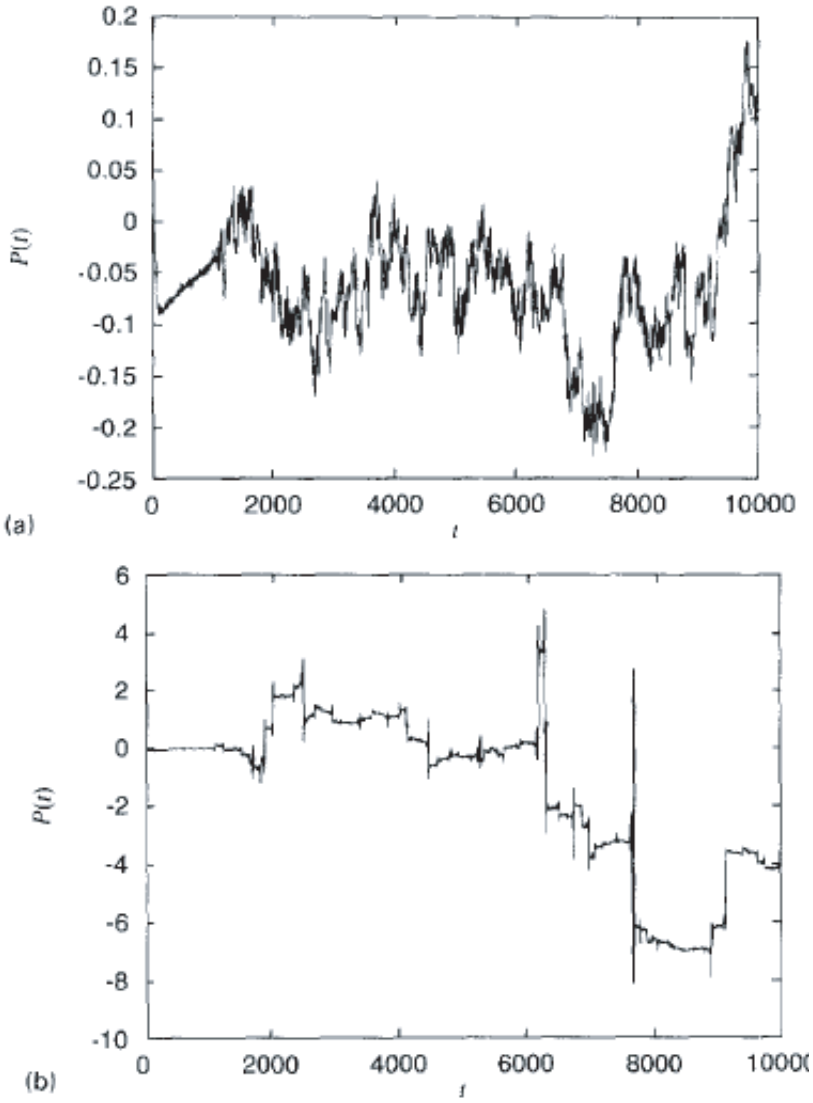

Figure 1.10: Examples of temporal fluctuations of the market price $P(t)$, simulated by the ST model: (a) $c = 0.0$; (b) $c = 0.3$. This graph is adapted from [29].

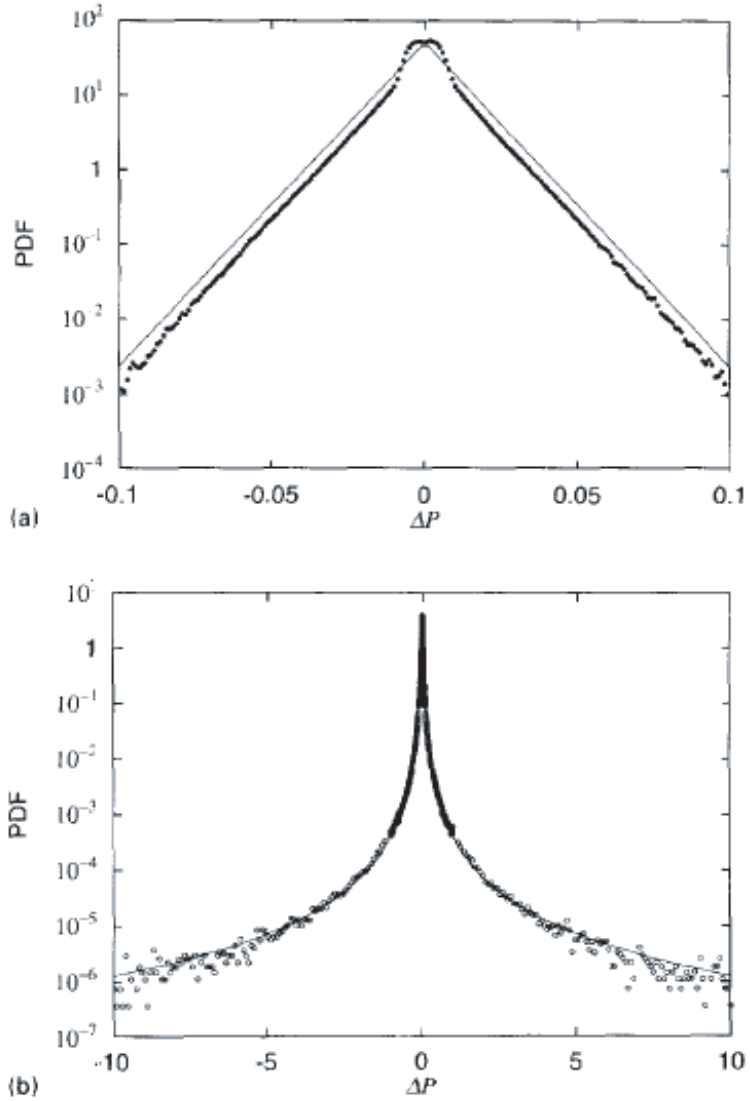

Figure 1.11: Semi-logarithmic plots of the probability density functions of ΔP, simulated by the ST model: (a) $c = 0.0$; (b) $c = 0.3$. The dots represent results of the numerical simulation and the lines represent theoretical curves: (a) a hybrid of Gaussian-Laplacian distribution, whose variance is 0.001; (b) a power-law distribution, $f(\Delta P) \propto (\Delta P)^{-2.5}$. This graph is adapted from [29].

Gopikrishnan *et al.* [8, 9] found the power-law behavior of the stock-price fluctuations only in the time interval greater than 16 [min]. However, in the highest resolution data (tick-by-tick data), the stock price change is essentially discrete and does not seem to obey a power law; it rather seems to obey a step-like function. Therefore, in the time scale shorter than 16 [min], there is a possibility that one may find in the stock-market fluctuation another 'law' which may not be a simple power law.

The author would like to make two notes on the power-law behavior. First, econophysics thus found new laws in economic systems and reproduced the financial phenomena by constructing various models. Although financial engineering can reproduce the power-law behavior of the price fluctuations by, for example, the famous GARCH [5, 33, 34] model, econophysics has constructed and is constructing various types of models from both microscopic and macroscopic viewpoints, aiming to find *universality* in economic systems.

Second, there is a possible mistake in analyzing the logarithm of the price change. Nowadays, analyzing the logarithm of the price change

$$G(t) = \ln \frac{Y(t)}{Y(t-T)} \tag{1.11}$$

is becoming the standard. An alternative way of analyzing the price change is to focus on the absolute change

$$\Delta Y(t) \equiv Y(t) - Y(t-T). \tag{1.12}$$

Substituting the equation (1.12) into (1.11), we obtain

$$G(t) = \ln \frac{Y(t-T) - \Delta Y(t)}{Y(t-T)} \tag{1.13}$$

$$= \ln \left(1 - \frac{\Delta Y(t)}{Y(t-T)} \right) \tag{1.14}$$

$$\simeq -\frac{\Delta Y(t)}{Y(t-T)} \tag{1.15}$$

for $\Delta Y(t) \ll Y(t-T)$. The absolute value of ΔY is usually of the order of 1% of the price Y for frequently traded stocks in Japan. Analyzing the quantity $G(t) = \ln(Y(t)/Y(t-T)) \simeq \Delta Y/Y$ may be dangerous, because its distribution obeys a power law even if, in the simplest case, $|\Delta Y|$ is a constant and hence Y is a normal random walk. Therefore we should be careful in analyzing the price fluctuation using the formula (1.11).

In the future, econophysics may be a part of financial engineering or classical economics. If it will be so, however, the efforts of econophysics, analyzing huge amount of high frequency financial data and modeling economic systems by using the concepts and methods developed in physics, will make an important part of the compound field. The position of econophysics as against to financial engineering and classical economics is just like that of quantum physics as against to classical physics or like that of statistical physics as against to thermodynamics.

From the physical viewpoint, the economic systems are, in some sense, ideal non-equilibrium open systems and strongly correlated many-body systems. We can obtain huge amount of electronic data to analyze without any experiments. Econophysics aims to analyze these data, find laws and understand the mechanisms of the laws. One day we may be able to import the harvests of the econophysics into the study in other physical complex systems.

1.6 The contents of the thesis

The aim of the thesis is to reproduce and understand an interaction among financial markets though triangular arbitrage in the foreign exchange market. In Chap. 2, we explain what is the triangular arbitrage transaction and analyze the feasibility of the transaction. In Chap. 3, we introduce a new model which reproduces the interaction among the foreign exchange rates well. We refer to this model as the *macroscopic* model because the model is phenomenological. We then show that the macroscopic model can explain a negative auto-correlation of the fluctuations of the foreign exchange rates. We explain that the correlation of the foreign exchange rates can appear without actual triangular arbitrage transactions. In Chap. 4, we introduce a new model which focuses on the dynamics of each dealer in the markets. We refer to this model as the *microscopic* model. The microscopic model also describes the interactions among the markets well. We explore the relation between the microscopic model and the macroscopic model.

Chapter 2

Triangular Arbitrage as an Interaction among Foreign Exchange Rates

2.1 Introduction

Analyzing correlation in financial time series is a topic of considerable interest [35]–[50]. In the foreign exchange market, a correlation among the exchange rates can be generated by a triangular arbitrage transaction. The triangular arbitrage is a financial activity that takes advantage of the three exchange rates among three currencies [51, 52, 53]. Suppose that we exchange one US dollar to some amount of Japanese yen, exchange the amount of Japanese yen to some amount of euro, and finally exchange the amount of euro back to US dollar; then how much US dollar do we have? There are opportunities that we have more than one US dollar. The triangular arbitrage transaction is the trade that takes this type of opportunities. It has been argued that the triangular arbitrage makes the product of the three exchange rates converge to a certain value [51]. In other words, the triangular arbitrage is a form of interaction among currencies.

The purpose of this chapter is to show that there is in fact triangular arbitrage opportunities in foreign exchange markets and they generate an interaction among foreign exchange rates. We analyze real data in Sec. 2.2,

The content of this chapter was published in: [52] Y. Aiba, N. Hatano, H. Takayasu, *et al.*, Physica A **310** (2002) 467–379.

showing that the product of three foreign exchange rates has a narrow distribution with fat tails.

2.2 Existence of triangular arbitrage opportunities

We analyze actual data of the yen-dollar rate, the yen-euro rate and the dollar-euro rate, taken from January 25 1999 to March 12 1999 except for weekends. We show in this section that there are actually triangular arbitrage opportunities and that the three exchange rates correlate strongly.

In order to quantify the triangular arbitrage opportunities, we define the quantity

$$\mu(t) = \prod_{x=1}^{3} r_x(t) \ , \tag{2.1}$$

where $r_x(t)$ denotes each exchange rate at time t. We refer to this quantity as the rate product. There is a triangular arbitrage opportunity whenever the rate product is greater than unity.

To be more precise, there are two types of the rate product. One is based on the arbitrage transaction in the direction of dollar to yen to euro to dollar. The other is based on the transaction in the opposite direction of dollar to euro to yen to dollar. Since these two values show similar behavior, we focus on the first type of $\mu(t)$ in the present and the next chapters. Thus, we specifically define each exchange rate as

$$r_1(t) \equiv \frac{1}{\text{yen-dollar ask } (t)} \tag{2.2}$$

$$r_2(t) \equiv \frac{1}{\text{dollar-euro ask } (t)} \tag{2.3}$$

$$r_3(t) \equiv \text{yen-euro bid } (t). \tag{2.4}$$

Here, 'bid' and 'ask,' respectively, represent the best bidding prices to buy and to sell in each market. We assume here that an arbitrager can transact instantly at the bid and the ask prices provided by information companies and hence we use the prices at the same time to calculate the rate product.

For later convenience, we also define the logarithm rate product ν as the

logarithm of the product of the three rates:

$$\nu(t) = \ln \prod_{x=1}^{3} r_x(t) = \sum_{x=1}^{3} \ln r_x(t). \tag{2.5}$$

There is a triangular arbitrage opportunity whenever this value is positive.

We can define another logarithm rate product ν', which has the opposite direction of the arbitrage transaction to ν, that is, from Japanese yen to euro to US dollar back to Japanese yen:

$$\nu'(t) = \sum_{x=1}^{3} \ln {r'}_x(t), \tag{2.6}$$

where

$${r'}_1(t) \equiv \text{ yen-dollar bid } (t) \tag{2.7}$$

$${r'}_2(t) \equiv \text{ dollar-euro bid } (t) \tag{2.8}$$

$${r'}_3(t) \equiv \frac{1}{\text{yen-euro ask } (t)}. \tag{2.9}$$

This logarithm rate product ν' will appear in Chap. 4.

Figure 2.1(a)-(c) shows the actual changes of the three rates: the yen-euro ask, the dollar-euro ask and the yen-euro bid. Figure 2.1(d) shows the behavior of the rate product $\mu(t)$. We can see that the rate product μ fluctuates around the average

$$m \equiv \langle \mu(t) \rangle \simeq 0.99998. \tag{2.10}$$

(The average is less than unity because of the spread; the spread is the difference between the ask and the bid prices and is usually of the order of 0.05% of the prices.) The probability density function of the rate product μ (Fig. 2.2) has a sharp peak and fat tails while those of the three rates (Fig. 2.3) do not. It means that the fluctuations of the exchange rates have correlation that makes the rate product converge to the average m.

2.3 Feasibility of the triangular arbitrage transaction

We discuss here the feasibility of the triangular arbitrage transaction. We analyze the duration of the triangular arbitrage opportunities and calculate

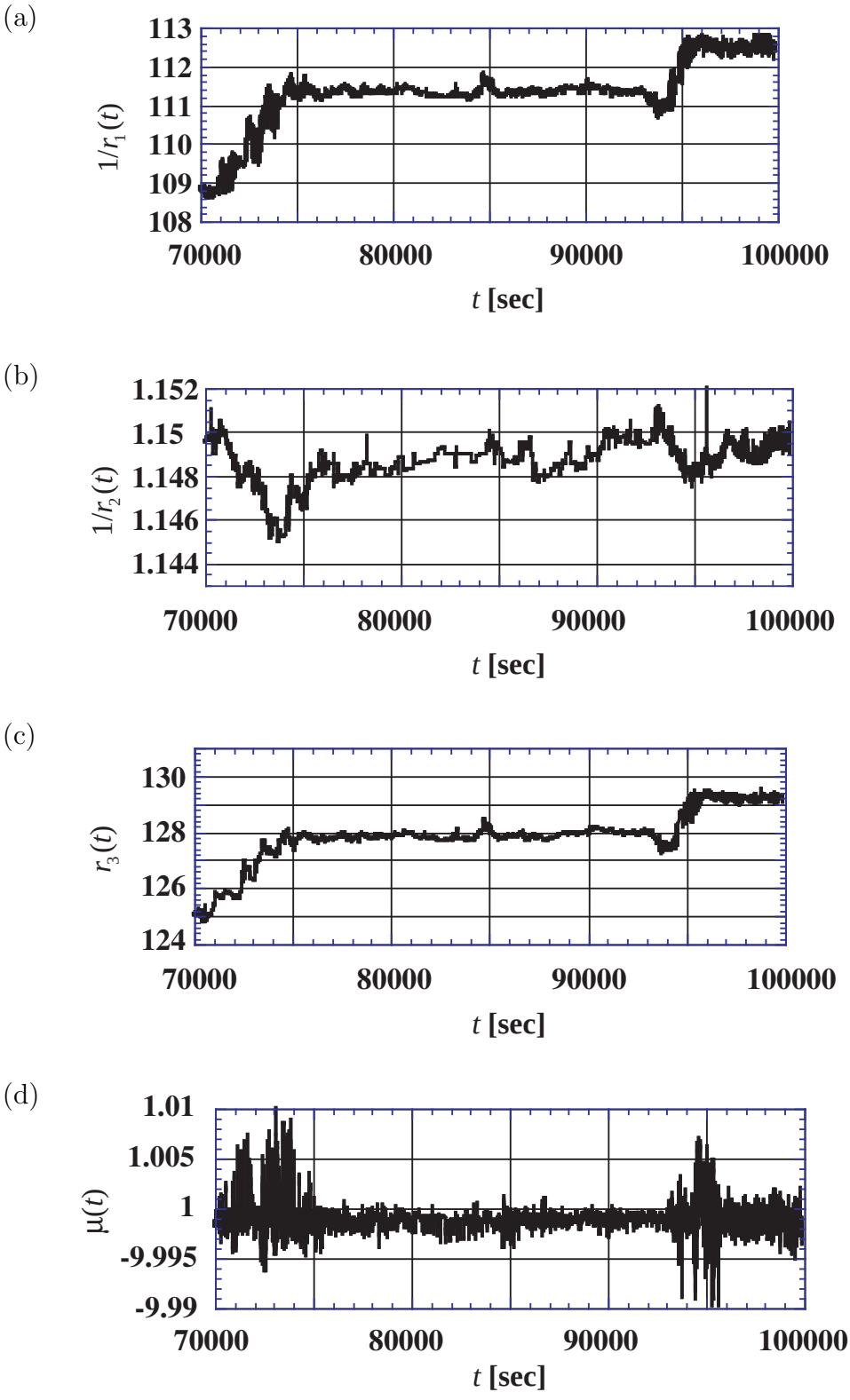

Figure 2.1: The time dependence of (a) the yen-dollar ask $1/r_1$, (b) the dollar-euro ask $1/r_2$, (c) the yen-euro bid r_3 and (d) the rate product μ. The horizontal axis denotes the seconds from 00:00:00, January 12 1999.

(a)

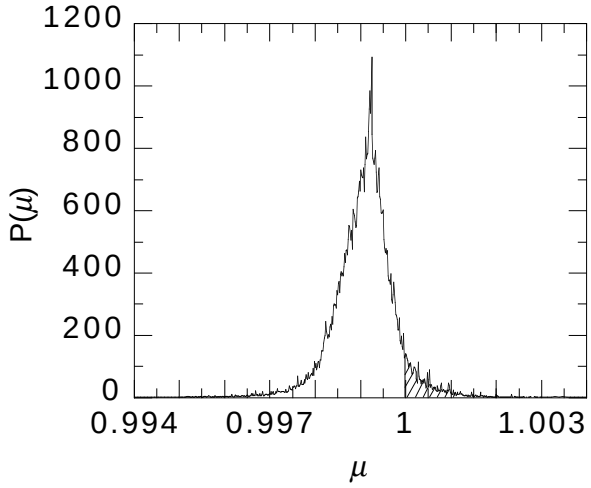

(b)

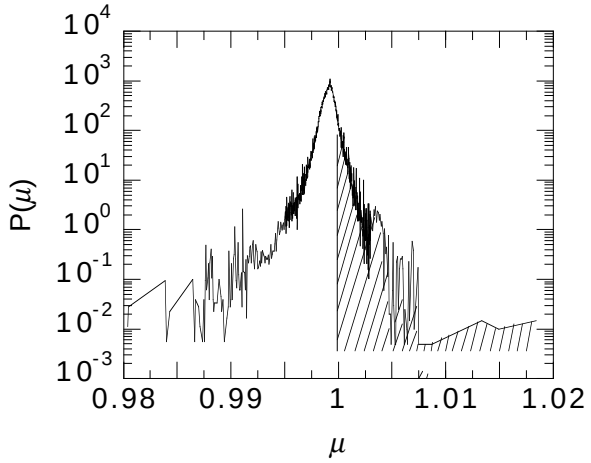

Figure 2.2: The probability density function of the rate product μ. (b) is a semi-logarithmic plot of (a). The shaded area represents triangular arbitrage opportunities. The data were taken from January 25 1999 to March 12 1999.

(a)

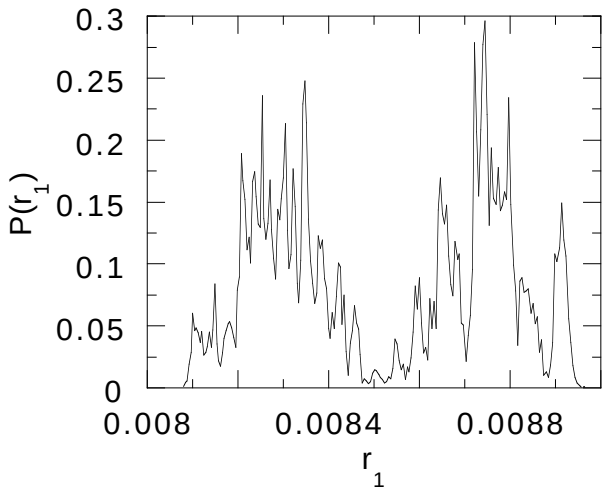
0.3
0.25
0.2
0.15
0.1
0.05
0
P(r1)
0.008
0.0084
0.0088
r1

(b)

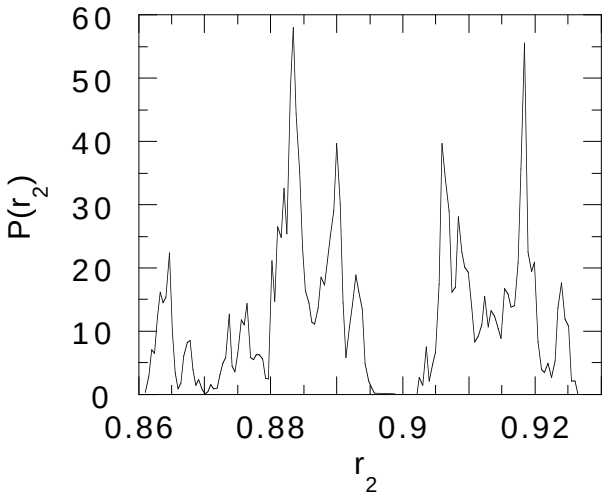
60
50
40
30
20
10
0
P(r2)
0.86
0.88
0.9
0.92
r2

(c)

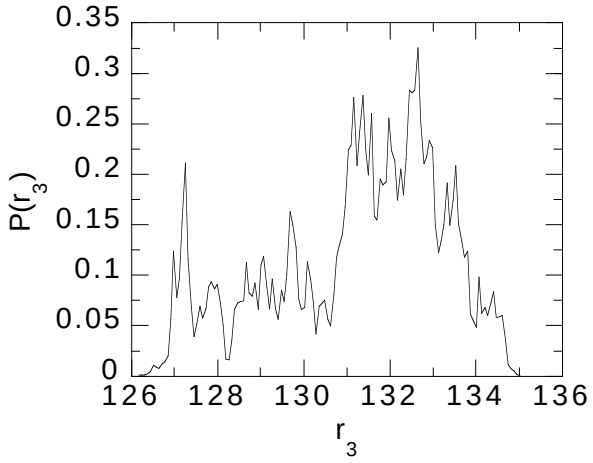

Figure 2.3: The probability density function of the three rates: (a) the reciprocal of the yen-dollar ask, r_1, (b) the reciprocal of the dollar-euro ask, r_2 and (c) the yen-euro bid r_3. The data were taken from January 25 1999 to March 12 1999.

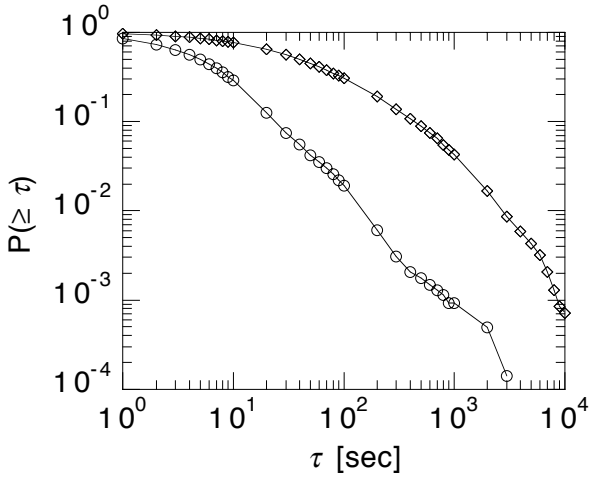

Figure 2.4: The cumulative distributions of τ_+ ($\circ$) and τ_- ($\diamond$). The distribution of τ_+ shows a power-low behavior. The data were taken from January 25 1999 to March 12 1999.

whether an arbitrager can make profit or not.

The shaded area in Fig. 2.2 represents triangular arbitrage opportunities. We can see that the rate product is grater than unity for about 6.4% of the time. It means that triangular arbitrage opportunities exist about ninety minutes a day. The ninety minutes, however, include the cases where the rate product μ is greater than unity very briefly. The triangular arbitrage transaction is not feasible in these cases.

In order to quantify the feasibility, we analyze the duration of the triangular arbitrage opportunities. Figure 2.4 shows the cumulative distributions of the duration τ_+ of the situation $\mu > 1$ and τ_- of $\mu < 1$. It is interesting that the distribution of τ_+ shows a power-law behavior while the distribution of τ_- dose not. This difference may suggest that the triangular arbitrage transaction is carried out indeed.

In order to confirm the feasibility of the triangular arbitrage, we simulate the triangular arbitrage transaction using our time series data. We assume that it takes $T_{\rm rec}$[sec] for an arbitrager to recognize triangular arbitrage opportunities and $T_{\rm exe}$[sec] to execute a triangular arbitrage transaction; see Fig. 2.5. We also assume that the arbitrager transacts whenever the arbitrager recognizes the opportunities. Figure 2.6 shows how much profit the

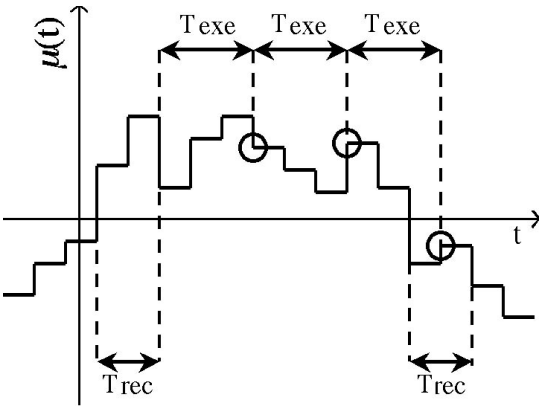

Figure 2.5: A conceptual figure of the profit calculation. We assume that it takes T_{rec}[sec] for an arbitrager to recognize triangular arbitrage opportunities and T_{exe}[sec] to execute a triangular arbitrage transaction. The circles ($\circ$) indicate the instances where triangular arbitrage transactions are carried out.

arbitrager can make from one US dollar (or Japanese yen or euro) in a day. We can see that the arbitrager can make profit if it takes the arbitrager a few seconds to recognize the triangular arbitrage opportunities and to execute the triangular arbitrage transaction.

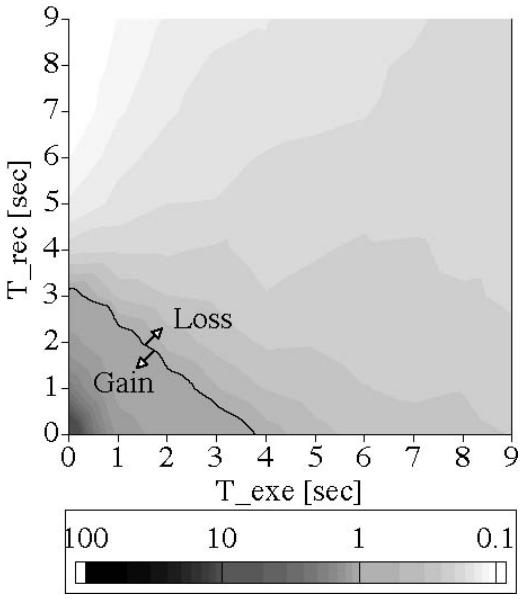

Figure 2.6: A phase diagram of the profit that an arbitrager can make from one US dollar (or Japanese yen or euro) in a day under the assumption shown in Fig. 2.5.

Chapter 3

A Macroscopic Model of Triangular Arbitrage Transaction

3.1 Macroscopic model of triangular arbitrage

We here introduce a new model that takes account of the effect of the triangular arbitrage transaction in the form of an interaction among the three rates. Many models of price change have been introduced so far: for example, the Lévy-stable non-Gaussian model [35]; the truncated Lévy flight [54]; the ARCH/GARCH processes [55, 56]. They discuss, however, only the change of one price. They did not consider an interaction among multiple prices. As we discussed in Sec. 2.2, however, the triangular arbitrage opportunity exists in the market and is presumed to affect price fluctuations in the way the rate product tends to converge to a certain value.

The content of this chapter was published in: [52] Y. Aiba, N. Hatano, H. Takayasu, K. Marumo, T. Shimizu, Physica A **310** (2002) 467–379; Y. Aiba, N. Hatano, H. Takayasu, K. Marumo, T. Shimizu, Physica A **324** (2003) 253–257; [57] Y. Aiba, N. Hatano, Physica A **344** (2004) 174–177; [58] Y. Aiba, N. Hatano, H. Takayasu, K. Marumo, T. Shimizu, in: H. Takayasu (Ed.) The Application of Econophysics, Proceedings of the Second Nikkei Symposium, Springer-Verlag Tokyo (2004) pp. 18–23.

3.1.1 Basic time evolution

The basic equation of our model is a time-evolution equation of the logarithm of each rate:

$$\ln r_x(t+T) = \ln r_x(t) + \eta_x(t) + g(\nu(t)), \quad (x = 1, 2, 3) \tag{3.1}$$

where ν is the logarithm rate product (2.5), and T is a time step which controls the time scale of the model; we later use the actual financial data every T[sec]. Just as μ fluctuates around $m = \langle \mu \rangle \simeq 0.99998$, the logarithm rate product ν fluctuates around

$$\epsilon \equiv \langle \ln \mu \rangle \simeq -0.00091 \tag{3.2}$$

(Fig. 3.1(a)). In this model, we focus on the logarithm of the rate-change ratio $\ln(r_x(t+T)/r_x(t))$, because the relative change is presumably more essential than the absolute change. We assumed in Eq. (3.1) that the change of the logarithm of each rate is given by an independent fluctuation $\eta_x(t)$ and an attractive interaction $g(\nu)$. The triangular arbitrage is presumed to make the logarithm rate product ν converge to the average ϵ; thus, the interaction function $g(\nu)$ should be negative for ν greater than ϵ and positive for ν less than ϵ:

$$g(\nu) \begin{cases} < 0 & , \quad \text{for } \nu > \epsilon \\ > 0 & , \quad \text{for } \nu < \epsilon. \end{cases} \tag{3.3}$$

As a linear approximation, we define $g(\nu)$ as

$$g(\nu) \equiv -k(\nu - \epsilon) \tag{3.4}$$

where k is a positive constant which specifies the interaction strength.

The time-evolution equation of ν is given by summing Eq. (3.1) over all x:

$$\nu(t+T) - \epsilon = (1 - 3k)(\nu(t) - \epsilon) + F(t), \tag{3.5}$$

where

$$F(t) \equiv \sum_{x=1}^{3} \eta_x(t). \tag{3.6}$$

This is our basic time-evolution equation of the logarithm rate product.

From a physical viewpoint, we can regard the model equation (3.1) as a one-dimensional random walk of three particles with a restoring force, by

(a)

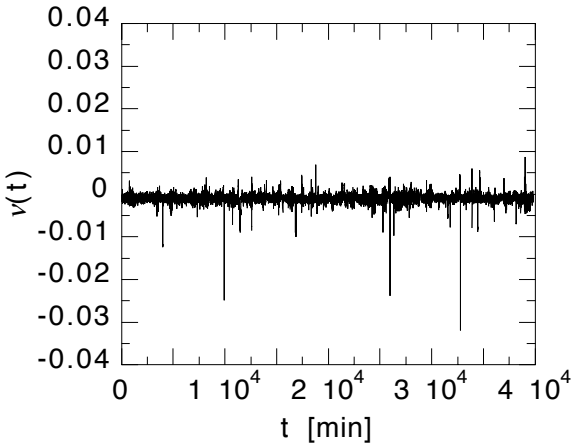

(b)

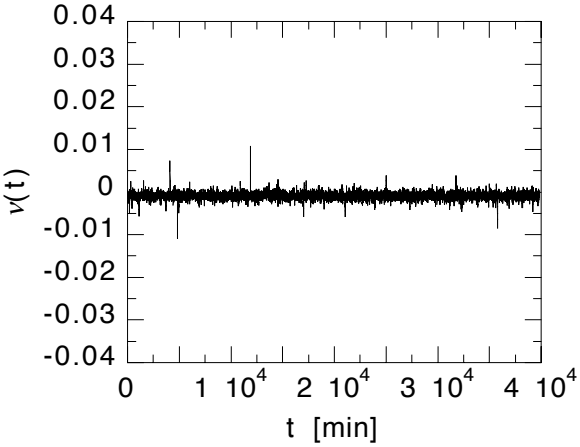

(c)

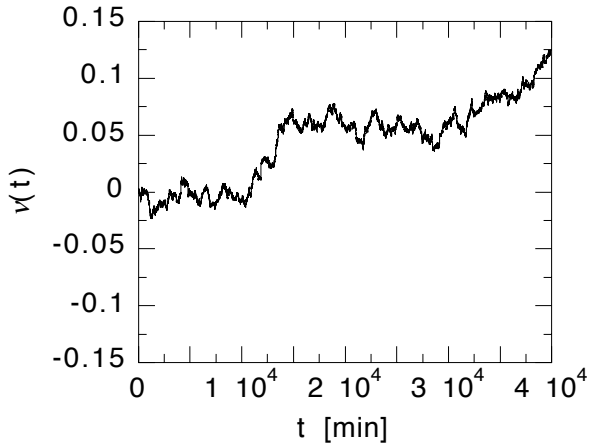

Figure 3.1: The time dependence of $\nu(t[\mathrm{min}])$ of (a) the real data, (b) the simulation data with the interaction and (c) without the interaction. In (b), ν fluctuates around ϵ like the real data.

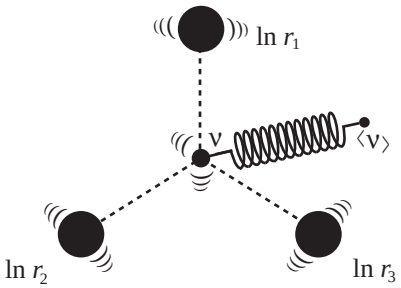

Figure 3.2: A schematic image of the model. The three random walkers with the restoring force working on the center of gravity.

interpreting $\ln r_x$ as the position of each particle (Fig. 3.2). The logarithm rate product ν is the summation of $\ln r_x$, hence is proportional to the center of gravity of the three particles. The restoring force $g(\nu)$ makes the center of gravity converge to a certain point $\langle\nu\rangle$. The form of the restoring force (3.4) is the same as that of the harmonic oscillator. Hence we can regard the coefficient k as a spring constant.

3.1.2 Estimation of parameters

The spring constant k is related to the auto-correlation function of ν as follows:

$$1 - 3k = c(T) \equiv \frac{\langle \nu(t+T)\nu(t)\rangle - \langle \nu(t)\rangle^2}{\langle \nu^2(t)\rangle - \langle \nu(t)\rangle^2}. \tag{3.7}$$

Using Eq. (3.7), we can estimate k from the real data series as a function of the time step T. The auto-correlation function $c(T)$ is shown in Fig. 3.3(a). The estimate of $k(T)$ is shown in Fig. 3.3(b). The spring constant k increases with the time step T. In the present chapter, we fix the time step at $T = 60$[sec] and hence use

$$k(1[\text{min}]) = 0.17 \pm 0.02 \tag{3.8}$$

for our simulation. We will come back to this point in Sec. 4.3.

On the other hand, the fluctuation of foreign exchange rates is known to be a fat-tail noise [59, 60]. Here we take $\eta_x(t)$ as the truncated Lévy process

(a)

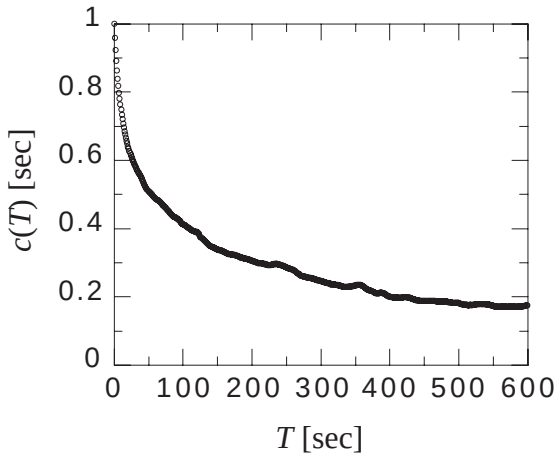

(b)

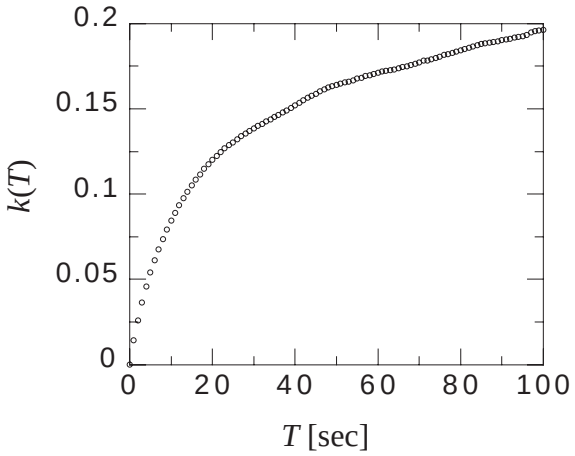

Figure 3.3: (a) The auto-correlation function of ν, $c(T)$. (b) The spring constant k as a function of the time step T. The spring constant k increases with the time step T.

rate	α	γ	l
r_1 (1/yen-dollar ask)	1.8	7.61×10^{-7}	1.38×10^{-2}
r_2 (1/dollar-euro ask)	1.7	4.06×10^{-7}	3.81×10^{-2}
r_3 (yen-euro bid)	1.8	6.97×10^{-7}	7.58×10^{-2}

Table 3.1: The estimates of the parameters.

[54, 61]

$$P_{\mathrm{TLF}}(\eta;\alpha,\gamma,l) = qP_{\mathrm{L}}(\eta;\alpha,\gamma)\Theta(l-|\eta|), \tag{3.9}$$
$$\tag{3.10}$$

where q is the normalization constant, $\Theta(x)$ represents the step function and $P_{\mathrm{L}}(x;\alpha,\gamma)$ is the symmetric Lévy distribution of index α and scale factor γ:

$$P_{\mathrm{L}}(x;\alpha,\gamma) = \frac{1}{\pi}\int_0^\infty e^{-\gamma|k|^\alpha}\cos(kx)\mathrm{d}k \quad 0<\alpha<2. \tag{3.11}$$

We determine the parameters α, γ and l by using the following relations for $1<\alpha<2$ [13, 59]:

$$c_2 = \frac{\alpha(\alpha-1)\gamma}{|\cos(\pi\alpha/2)|}l^{2-\alpha}, \tag{3.12}$$
$$\kappa = \frac{(3-\alpha)(2-\alpha)|\cos(\pi\alpha/2)|}{\alpha(\alpha-1)\gamma}l^{\alpha}, \tag{3.13}$$

where c_n denotes the nth cumulant and κ is the kurtosis $\kappa = c_4/{c_2}^2$. The estimates are shown in Table 3.1. The generated noises with the estimated parameters are compared to the actual data in Fig. 3.4.

We simulated the time evolution (3.5) with the parameters given in Eqs. (3.2), (3.8) and Table 1. The probability density function of the results (Fig. 3.1(b)) is compared to that of the real data (Fig. 3.1(a)) with $T = 1$[min] in Fig. 3.5. The fluctuation of the simulation data is consistent with that of the real data. In particular, we see good agreement around $\nu \simeq \epsilon$ as a result of the linear approximation of the interaction function. Figure 3.1(c) shows $\nu(t)$ of the simulation without the interaction, *i.e.* $k = 0$. The quantity ν fluctuates freely, which is inconsistent with the real data.

(a)

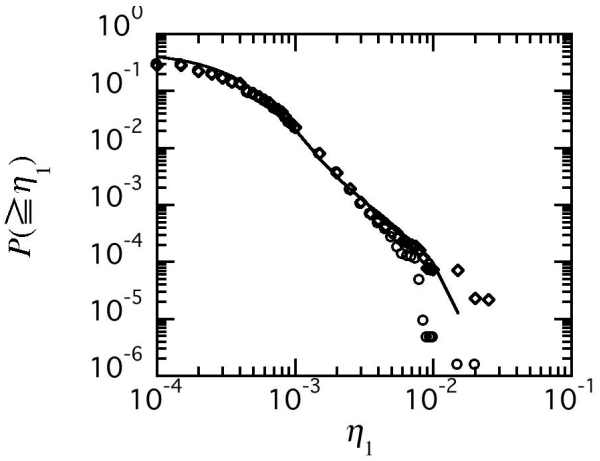

(b)

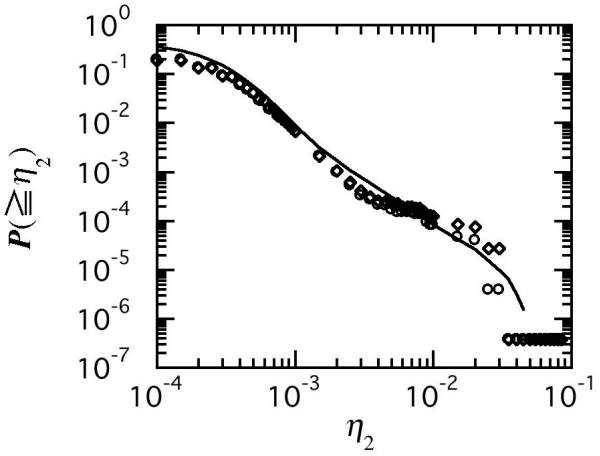

(c)

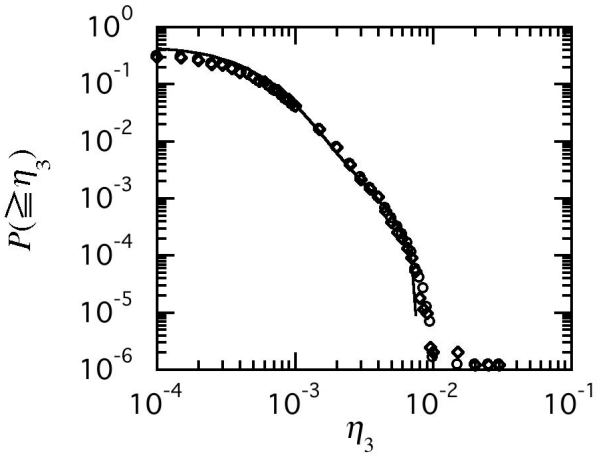

Figure 3.4: The cumulative distributions of one-minute changes $|\ln r_x(t + 1[\text{min}]) - \ln r_x(t)|$ ($\circ$ represents upward movements and $\diamond$ represents downward movements) and the generated noise η_x (—): (a) the yen-dollar ask and η_1, (b) the dollar-euro ask and η_2, and (c) yen-euro bid and η_3. The real data were taken from January 25 1999 to March 12 1999.

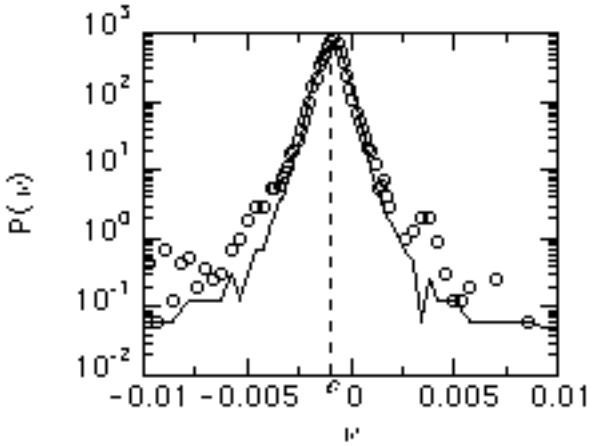

Figure 3.5: The probability density function of ν. The circle ($\circ$) denotes the real data and the solid line denotes our simulation data with the interaction. The simulation data fit the real data well.

3.1.3 Analytical approach

We can solve the time-evolution equation (3.5) analytically in some cases. Let us define

$$\omega(t) \equiv \nu(t) - \epsilon \tag{3.14}$$

and

$$\begin{cases} \omega = \omega(t), & \omega' = \omega(t+T), \\ F = F(t), & F' = F(t+T), \\ c = c(T). \end{cases} \tag{3.15}$$

Equation (3.5) is then reduced to

$$\omega' = c\omega + F \tag{3.16}$$

Assume that the probability of ω having a value in $\omega \sim \omega + \mathrm{d}\omega$ is $P_\omega(\omega)$. The joint probability of ω' having a value in $\omega' \sim \omega' + \mathrm{d}\omega'$ and F' having a value in $F' \sim F' + \mathrm{d}F'$ is given by

$$\begin{aligned} P_{\omega',F'}(\omega', F')\mathrm{d}\omega'\mathrm{d}F' &= P_\omega(\omega)P_F(F')\mathrm{d}\omega\mathrm{d}F' \\ &= \frac{1}{c}P_\omega(\frac{\omega' - F'}{c})P_F(F')\mathrm{d}\omega'\mathrm{d}F', \end{aligned} \tag{3.17}$$

where $P_F(F)$ is the probability of F having a value in $F \sim F + \mathrm{d}F$. The probability density function of ω' is thus given by

$$P_{\omega'}(\omega') = \frac{1}{c}\int P_{\omega}(\frac{\omega' - F'}{c})P_F(F')\mathrm{d}F'. \tag{3.18}$$

The characteristic function of ω' is the Fourier transform

$$\tilde{P}_{\omega'}(\theta) = \int P_{\omega'}(\omega')e^{i\omega'\theta}\mathrm{d}\omega' = \tilde{P}_{\omega}(c\theta)\tilde{P}_F(\theta), \tag{3.19}$$

where $\tilde{P}_{\omega}$ and $\tilde{P}_F$ are the Fourier transforms of P_{ω} and P_F, respectively. Then we obtain

$$\begin{aligned}
\tilde{P}_{\omega(t)}(\theta) &= \tilde{P}_{\omega(t-T)}(c\theta)\tilde{P}_{F(t-T)}(\theta) \\
&= \tilde{P}_{\omega(0)}(c^N\theta)\prod_{n=0}^{N}\tilde{P}_F(c^n\theta) \\
&= \tilde{P}_{\omega(0)}(c^N\theta)\prod_{x=1}^{3}\prod_{n=0}^{N}\tilde{P}_{\eta_x}(c^n\theta) \\
&= \prod_{x=1}^{3}\prod_{n=0}^{N}\tilde{P}_{\eta_x}(c^n\theta),
\end{aligned} \tag{3.20}$$

where $t = NT$. We here assumed $P_{\omega(0)}(\omega) = \delta(\omega)$ and hence $\tilde{P}_{\omega(0)}(\theta) = 1$.

The above argument shows the essential reason of the sharp peak and fat tails in Fig. 2.2. If we had $c = 1$, or $k = 0$ (without the interaction), the noise F at every time step would accumulate in ω and the probability density function of $\omega = \nu - \epsilon$ would be Gaussian due to the central limit theorem. If we have $c < 1$, or $k > 0$ (with the interaction), the noise at the past time steps decay as c^n. The largest contribution to ω comes from the noise one time step before, which is a fat-tail noise [54].

As a special case, if the noises $\eta_x(t)$ obey a Lévy distribution of the same index α and the same scale factor γ, namely if

$$\tilde{P}_{\eta_x}(\theta) = e^{-\gamma|\theta|^{\alpha}} \quad \text{for all } x, \tag{3.21}$$

the distribution of ω is also a Lévy distribution of the same index α and a different scale factor γ' given by

$$\gamma' = \frac{3}{1 - \{c(T)\}^{\alpha}}\gamma. \tag{3.22}$$

3.2 Negative auto-correlation of the foreign exchange rates in a short time scale

We point out another consequence of the triangular arbitrage, namely the negative auto-correlation of each exchange rate in a short time scale. Let us first show it in the actual data. We analyzed actual tick-by-tick data of the yen-dollar rate, the dollar-euro rate and the yen-euro rate, taken from January 25, 1999 to March 12, 1999 except for the weekends.

The auto-correlation function of the rate fluctuation is defined by the following formula:

$$c_x(n) = \frac{\langle \Delta r_x(t+nT)\Delta r_x(t)\rangle - \langle \Delta r_x(t)\rangle^2}{\langle \Delta r_x(t)^2\rangle - \langle \Delta r_x(t)\rangle^2}, \quad (x = 1, 2, 3; n = 0, 1, 2, ...), \tag{3.23}$$

where

$$\Delta r_x(t) \equiv \ln \frac{r_x(t+T)}{r_x(t)} \ (x = 1, 2, 3), \tag{3.24}$$

and the angular brackets $\langle \cdots \rangle$ denote the time average. We fixed the time step T at one minute.

Figure 3.6 shows that the auto-correlation function of each rate has a negative value for $n = 1$. We here claim that the triangular arbitrage is one of the major causes of this negative auto-correlation. In order to see it, we simulated Eq. (3.1) and calculated the auto-correlation function (3.23). The simulation data (also shown in Fig. 3.6) are qualitatively consistent with the behavior of the auto-correlation function of the actual data.

Another analysis is possible. Using Eqs. (2.5) and (3.1)-(3.6), we can rewrite the auto-correlation function (3.23) for $n = 1$ as

$$c_x(n=1) = \frac{\langle (\eta_x(t+T) + g(t+T))(\eta_x(t) + g(t))\rangle - \langle \eta_x(t) + g(t)\rangle^2}{\langle (\eta_x(t) + g(t))^2\rangle - \langle \eta_x(t) + g(t)\rangle^2} \tag{3.25}$$

$$= -k\frac{\sigma_{\eta_x}^2 - k(1-3k)\sigma_\nu^2}{\sigma_{\eta_x}^2 + k^2\sigma_\nu^2}, \tag{3.26}$$

where ${\sigma_x}^2$ denotes the variance of the variable x. We here used the following relations:

$$\langle \eta_x(t)\rangle = 0, \tag{3.27}$$

$$\langle \eta_x(t+T)\eta_x(t)\rangle = 0. \tag{3.28}$$

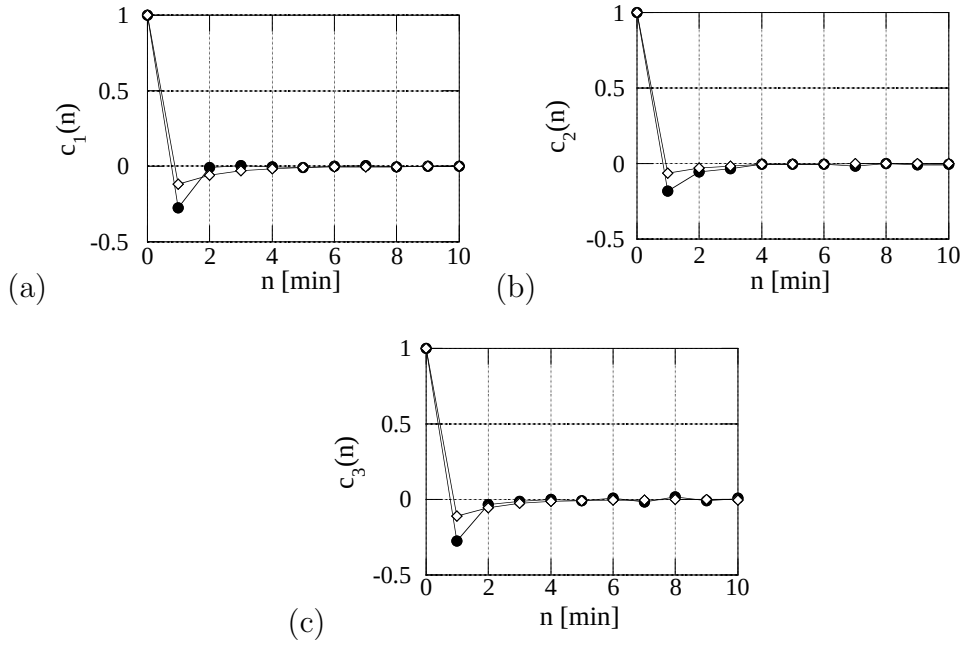

Figure 3.6: The auto-correlation function of the rate change of the actual data: (a) $c_1(n)$; (b) $c_2(n)$; (c) $c_3(n)$. The circles ($\circ$) denote the actual data and the diamonds ($\diamond$) denote the simulation data.

Table 3.2: The value of $c_x(n=1)$ from the actual data, the simulation data and Eq. (3.26).

Rate	Actual Data	Simulation	Eq. (3.26)
r_1 (1/yen-dollar ask)	-0.27	-0.12	-0.12
r_2 (1/dollar-euro ask)	-0.18	-0.061	-0.095
r_3 (yen-euro bid)	-0.28	-0.11	-0.13

Note that we have $c_x(n=1) \approx -k < 0$ for small k.

We can estimate σ_ν and σ_{η_x} from the market data. The auto-correlation function for $n=1$ thus-estimated is compared in Table 3.2 to the one from the actual data and the one from the simulation data.

The value of $c_x(n=1)$ from the actual data is less than those from the simulation data and Eq. (3.26). This may suggest that there are contributions from the triangular arbitrage of other combinations of three rates; for example, the triangular arbitrage among Japanese yen, US dollar and British pound.

3.3 What makes the rate product converge

The feasibility of the triangular arbitrage transaction is of much interest for financial-market practitioners and researchers. In Sec. 2.2, we discussed the feasibility of the transaction and concluded that the transaction is quite possible, by analyzing the high-frequency data [52]. Unfortunately, evidence for the actual occurrence of the transaction is not available to us. We nevertheless claim that the correlation can be generated even without actual triangular arbitrage transactions. Even if there is actually no triangular arbitrage transactions, the rate product should converge to unity. (Note, however, that we are not claiming that the transaction is infeasible.)

Consider the following situation: an international company wants to obtain Japanese Yen (JPY). The company has both Euro (EUR) and U.S. Dollar (USD). The exchange rates are:

$$1[\text{JPY}] = r_1[\text{USD}],\ 1[\text{USD}] = r_2[\text{EUR}] \text{ and } 1[\text{EUR}] = r_3[\text{JPY}].$$

Should the company sell Euro or U.S. Dollar to obtain Japanese Yen? It

costs r_1[USD] to buy one Japanese yen. If the company sells Euro, on the other hand, it costs

$$1[\text{JPY}] = \frac{1}{r_3}[\text{EUR}] = \frac{1}{r_2 r_3}[\text{USD}].$$

In order to make the cost lower, the company compares the value r_1 with $1/r_2 r_3$. It means that they compare the rate product μ in Eq. (2.1) with unity. When $r_1 > 1/r_2 r_3$, or $\mu > 1$, this is the situation of the triangular arbitrage opportunity, hence the company sells Euro and buys Japanese Yen. This transaction increases the demand of Japanese Yen against Euro and hence makes the JPY-EUR rate r_3 converge to the neutral one. Thus, the rate product μ converges to unity.

In the above example, the company needs to obtain Japanese Yen by selling Euro or U.S. Dollar. In the actual market, there are also companies which need to obtain Euro or U.S. Dollar by selling the other two currencies. They choose their trading strategies so as to avoid losses. The trading based on these strategies generates the correlation among foreign exchange rates. In this way, the three rates keep a certain relation without the triangular arbitrage transaction itself.

Chapter 4

A Microscopic Model of Triangular Arbitrage Transaction

4.1 Introduction

In Chap. 2, we pointed out the existence of the triangular arbitrage opportunity in the foreign exchange market and showed that the triangular arbitrage transaction makes the product of the three foreign exchange rates converge to its average, thereby generating an interaction among the rates. In order to study effects of the triangular arbitrage on the fluctuations of the exchange rates, in the previous chapter, we introduced a stochastic model (3.1) describing the time evolution of the exchange rates with an interaction. The model successfully describs the fluctuation of the data of the real market. The model is phenomenological; *i.e.* it treats the fluctuations of the rates as fluctuating particles and the interaction among the rates as a spring. We refer to this model as the 'macroscopic model' hereafter.

The purpose of this chapter is to understand *microscopically* effects of the triangular arbitrage on the foreign exchange market. For the purpose, we introduce a new model which focuses on each dealer in the markets; we refer to the new model as the 'microscopic model' hereafter. We then show the relation between the macroscopic model and the microscopic model through an interaction strength which is regarded as a spring constant.

The content of this chapter is in preparation for submission.

This chapter is organized as follows. In Sec. 4.2, we introduce the microscopic model which focuses on the dynamics of each dealer in the markets. The model reproduces the interactions among the markets well. We explore the relation between the spring constant of the macroscopic model and the parameters in the microscopic model in Sec. 4.3.

4.2 Microscopic model of triangular arbitrage

We here introduce a microscopic model which describes interactions among foreign exchange markets. The model focuses on the dynamics of each dealer in the market.

In order to describe each foreign exchange market microscopically, we use Sato and Takayasu's dealer model (the ST model; see Sec. 1.4.2) [29], which reproduces the power-law behavior of price changes in a single market well. Although we focus on the interactions among three currencies, two of the three markets can be regarded as one effective market [62]; *i.e.* the yen-euro rate and the euro-dollar rate are combined to an effective yen-dollar rate. In terms of the macroscopic model, we can redefine a variable r_2 as the product of r_2 and r_3. Then the renormalized variable r_2 follows a similar time-evolution equation. We therefore describe triangular arbitrage opportunities with only two interacting ST models, in order to simplify the situation.

4.2.1 Microscopic model of triangular arbitrage: interacting two systems of the ST model

We describe our microscopic model as a set of the ST models. In order to reproduce effects of the triangular arbitrage, we prepare two systems of the ST model, the market X and the market Y. As is noted above, we prepare only two markets to reproduce the effect of the triangular arbitrage because we regard two of the three markets as one effective market. Note that we can reproduce the markets interaction by preparing all of the three markets.

The dealers in the markets X and Y change their bidding prices according to the ST model as follows:

$$B_{i,X}(t+1) = B_{i,X}(t) + a_{i,X}(t) + c\Delta P_X(t) \text{ and} \tag{4.1}$$
$$B_{i,Y}(t+1) = B_{i,Y}(t) + a_{i,Y}(t) + c\Delta P_Y(t), \tag{4.2}$$

where X and Y denote the markets X and Y, respectively. An intra-market transaction takes place when the condition

$$\max\{B_{i,x}(t)\} \geq \min\{S_{i,x}\}, \quad x = X \text{ or } Y \tag{4.3}$$

is satisfied. We assume that Λ is common to the two markets. The price $P_x(t)$ is renewed in analog to the ST model:

$$P_x(t) = \begin{cases} (\max\{B_{i,x}(t)\} + \min\{S_{i,x}(t)\})/2, & \text{if the condition (4.3) is satisfied,} \\ P_x(t-1), & \text{otherwise,} \end{cases} \tag{4.4}$$

where $x = X$ or Y.

We here add a new *inter*-market transaction rule which makes the systems interact. The arbitrage transaction can take place when one of the conditions

$$\nu_X \equiv \max\{B_{i,X}(t)\} - (\min\{B_{i,Y}(t)\} + \Lambda) \geq 0 \tag{4.5}$$

$$\nu_Y \equiv \max\{B_{i,Y}(t)\} - (\min\{B_{i,X}(t)\} + \Lambda) \geq 0 \tag{4.6}$$

is satisfied (see Fig. 4.1). When the conditions (4.3) and (4.5) or (4.6) are both satisfied simultaneously, the condition (4.3) precedes.

Note that the arbitrage conditions $\nu_X \geq 0$ and $\nu_Y \geq 0$ in the microscopic model correspond to the arbitrage condition $\nu \geq 0$ in the actual market, where ν is defined by the equation (2.5). We assume that the dealers' bidding prices $\{B_i\}$ and $\{S_i\}$ correspond to the logarithm of the exchange rate, $\ln r_i$. Therefore, $\max\{B_{i,X}\}$ may be equivalent to $-\ln$(yen-dollar ask) while $\min\{S_{i,Y}\}$ may be equivalent to ln(dollar-euro ask) $-$ ln(yen-euro bid), and hence ν_X may be equivalent to ν. More precisely, the direction of the arbitrage transaction determines which of the quantities, ν_X or ν_Y, corresponds to the logarithm rate product ν. There are two directions of the triangular arbitrage transaction. The definition (2.5) specifically has the direction of Japanese yen to US dollar to euro to Japanese yen. As is mentioned in Sec. 2.2, we can define another logarithm rate product ν' in the actual market which has the opposite direction to ν, Japanese yen to euro to US dollar to Japanese yen. Hence, if the logarithm rate product ν in the actual market corresponds to ν_X in the equation (4.5), ν' corresponds to $-\nu_Y$ in the equation (4.6).

The procedures of the simulation of the microscopic model are as follows (Fig. 4.1):

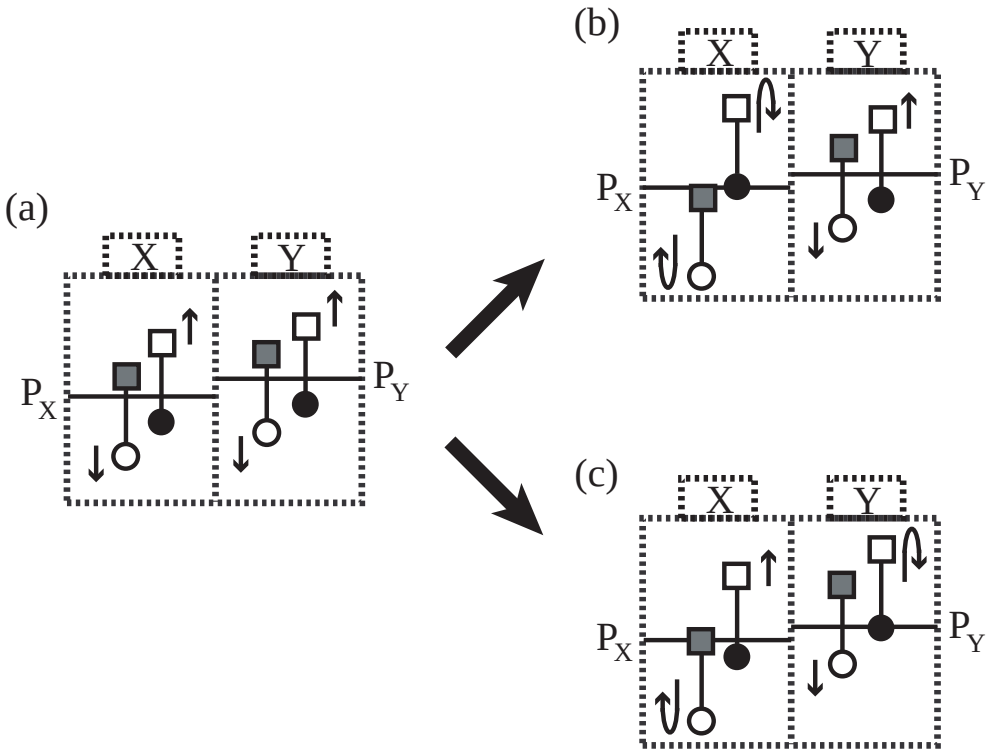

Figure 4.1: A schematic image of the transactions. Only the best bidders in the markets are illustrated, in order to simplify the image. The circles and the squares denote the dealers' bidding price to buy and to sell. The filled circles denote the best bidding prices to buy in the markets, $\max\{B_{i,X}\}$ and $\max\{B_{i,Y}\}$, and the gray squares denote the best bidding prices to sell in the markets, $\min\{B_{i,X}\} + \Lambda$ and $\min\{B_{i,Y}\} + \Lambda$. In the case (a), any of the conditions (4.3), (4.5) and (4.6) are not satisfied. The buyers move their prices up, and the sellers move their prices down. In the case (b), the dealers in the market X satisfy the condition (4.3); hence the intra-market transaction takes place. The price in the market X, P_X, is renewed, and the buyer and the seller of the transaction become a seller and a buyer, respectively. In the case (c), the seller in the market X and the buyer in the market Y satisfy the condition (4.6); hence the arbitrage transaction takes place. The price P_X in the market X becomes $\min\{B_{i,X}\} + \Lambda$, and the price P_Y in the market Y becomes $\max\{B_{i,Y}\}$. The buyer and the seller of the transaction become a seller and a buyer, respectively. The arbitrage transaction thus makes the interaction between the markets X and Y.

1. Prepare two systems of the ST model, the market X and the market Y, as described in Sec. 1.4.2. The parameters are common to the two systems.

2. Check the condition (4.3) and renew the prices by Eq. (4.4). If the condition (4.3) is satisfied, skip the step 3 and proceed to the step 4. Otherwise, proceed to the step 3.

3. Check the arbitrage conditions (4.5) and (4.6). If the condition (4.5) is satisfied, renew the prices $P_X(t)$ and $P_Y(t)$ to $\max\{B_{i,X}(t)\}$ and $\min\{B_{i,Y}(t)\} + \Lambda$, respectively. If the condition (4.6) is satisfied, renew the prices $P_X(t)$ and $P_Y(t)$ to $\min\{B_{i,X}(t)\}+\Lambda$ and $\max\{B_{i,Y}(t)\}$, respectively. If both of the conditions in (4.5) and (4.6) are satisfied, choose one of them with the probability of 50% and carry out the arbitrage transaction as described just above. If the arbitrage transaction takes place, proceed to the step 4; otherwise skip the step 4 and proceed to the step 5.

4. Calculate the difference between the new prices and the previous prices, $\Delta P_X(t) = P_X(t) - P_X(t-1)$ and $\Delta P_Y(t) = P_Y(t) - P_Y(t-1)$, and use them in Eqs. (4.1) and (4.2), respectively. Change the buyer and the seller of the transaction to a seller and a buyer, respectively. In other words, change the signs of $a_{i,X}$ and $a_{i,Y}$ of the dealers who transacted.

5. If any of the conditions (4.3), (4.5) and (4.6) are not satisfied, maintain the previous prices, $P_X(t) = P_X(t-1)$ and $P_Y(t) = P_Y(t-1)$, as well as the previous price differences, $\Delta P_X(t) = \Delta P_X(t-1)$ and $\Delta P_Y(t) = \Delta P_Y(t-1)$.

6. Change the dealers' bidding prices following Eqs. (4.1) and (4.2).

7. Repeat the steps from 2 to 6.

The quantities ν_X and ν_Y are shown in Fig. 4.2. (The parameters are common to the two markets X and Y: $N = 100$, $\alpha = 0.01$ and $\Lambda = 1.0$, which follows Ref. [29].) In Fig. 4.2(b) for $c = 0.3$, the fat-tail behavior of the price difference ν_X is consistent with the actual data as well as with the macroscopic model. Furthermore, ν_X reproduces the skewness of the actual data, which cannot be reproduced by the macroscopic model (Fig. 4.3). Note that the skewness of ν_Y is consistent with the behavior of ν'.

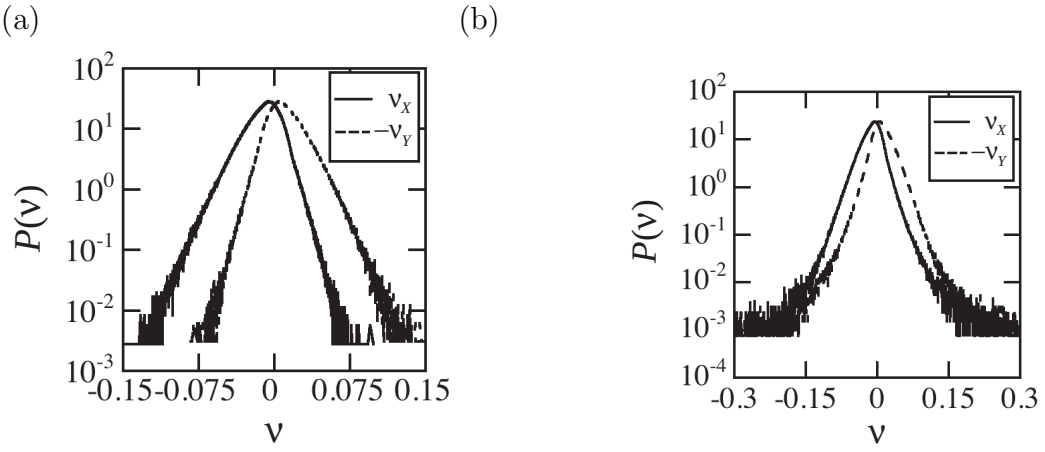

Figure 4.2: The distributions of ν_X and $-\nu_Y$. The parameters are fixed to $N = 100$, $\alpha = 0.01$, $\Lambda = 1.0$ and (a) $c = 0.0$, (b) $c = 0.3$, and are common to the market X and the market Y. The solid line denotes ν_X and the dashed line denotes ν_Y in each graph.

4.3 The microscopic parameters and the macroscopic spring constant

In this section, we discuss the relation between the macroscopic model and the microscopic model through the interaction strength, or the spring constant k.

In the microscopic model, we define the spring constant k_{micro}, which corresponds to the spring constant k of the macroscopic model, as follows:

$$k_{\text{micro}} \equiv \frac{1}{2}\left(1 - \frac{\langle \nu_X(t+1)\nu_X(t)\rangle - \langle \nu_X(t)\rangle^2}{\langle \nu_X(t)^2\rangle - \langle \nu_X(t)\rangle^2}\right). \tag{4.7}$$

Figure 4.4 shows the estimate (4.7) as a function of several parameters.

Remember that, in the macroscopic model, the spring constant k depends on the time step T (see Fig. 3.3(b)). The spring constant of the microscopic model k_{micro} also depends on a time scale as follows. The time scale of the ST model may be given by the following combination of the parameters [29]:

$$\langle n\rangle \simeq \frac{3\Lambda}{N\alpha}, \tag{4.8}$$

(a) (b)

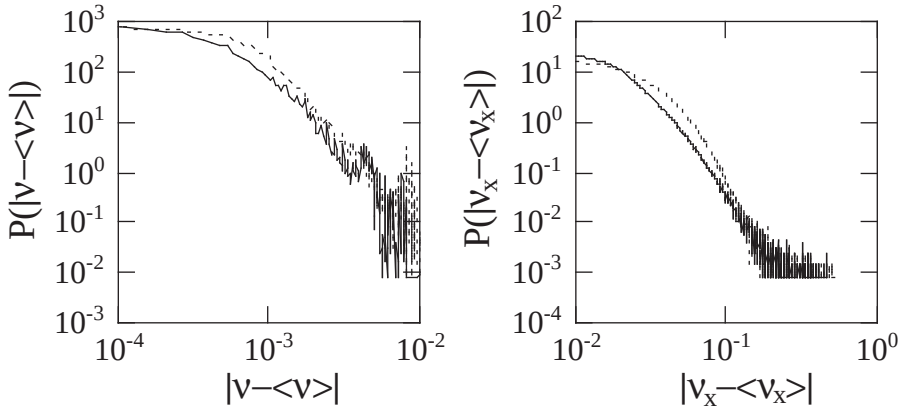

Figure 4.3: The probability distribution of the difference between the logarithm rate product and its average for (a) the actual data, $|\nu - \langle\nu\rangle|$ and for (b) the data of the microscopic model, $|\nu_x - \langle\nu_x\rangle|$ for $c = 0.3$. The solid lines represent the part in which the difference is positive and the dotted lines represent the part in which the difference is negative, in the both graphs. We can see that the probability distribution of the logarithm rate product ν has a skewness around its average, and the microscopic model qualitatively reproduces it well.

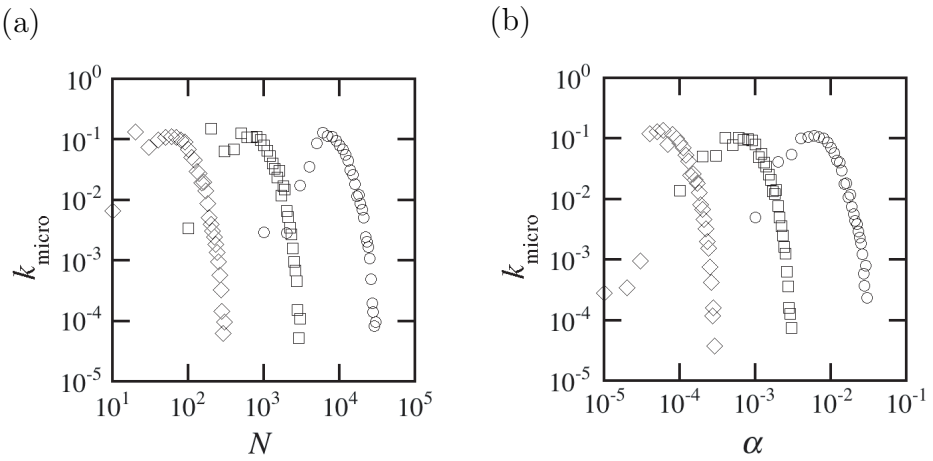

Figure 4.4: The spring constant k_{micro} as a function of parameters. The panel (a) shows the dependence on N. The other parameters are fixed to $\Lambda = 1.0$ and $\alpha = 0.0001, 0.001$ and 0.01 for the circles, the squares and the diamonds, respectively, and $c = 0.3$ for the all plots. The panel (b) shows the dependence on α. The other parameters are fixed to $\Lambda = 1.0$ and $N = 100, 1000$ and 10000 for the circles, the squares and the diamonds, respectively, and $c = 0.3$ for the all plots.

(a) (b)

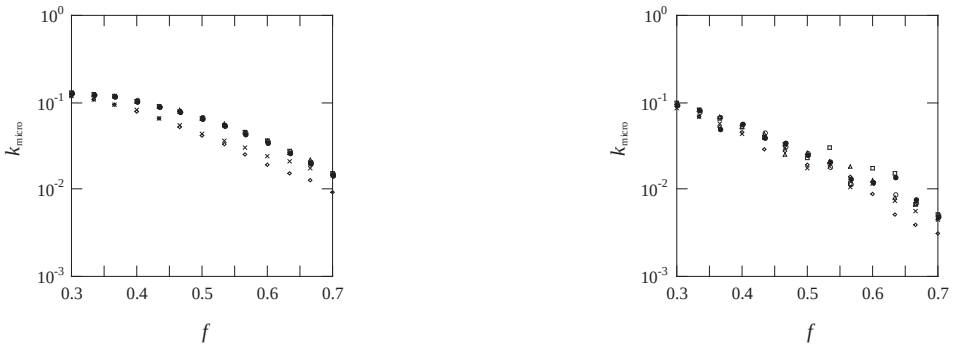

Figure 4.5: The scaling plot of the spring constant k_{micro} as a function of the trade frequency $f = N\alpha/3\Lambda$. The vertical axes are displayed in the logarithmic scale. The dealers' response to the price change, c, is fixed to 0.0 in (a) and 0.3 in (b). We fix $\alpha = 0.0001, 0.001$ and 0.01 and change N (open circles, squares, and diamonds, respectively) and $N = 100, 1000$ and 10000 and change α (crosses, filled circles and triangles, respectively), while Λ is fixed to 1. Note that all points collapse onto a single curve. The spring constant k_{micro} is scaled by f, and decays exponentially in both of the plots (a) and (b).

where n denotes the interval between two consecutive trades. Hence, the inverse of the equation (4.8),

$$f \equiv 1/\langle n \rangle \simeq \frac{N\alpha}{3\Lambda}, \tag{4.9}$$

is the frequency of the trades.

Although there are four parameters N, α, Λ and c, we change only three parameters N, α, and c and set $\Lambda = 1.0$, because only the ratios N/Λ and α/Λ are relevant in this system. The ratio N/Λ controls the density of the dealers and α/Λ controls the speed of the dealers' motion on average. Hence, we set $\Lambda = 1.0$ and change the other parameters hereafter.

We plot the spring constant k_{micro} as a function of the trade frequency $f \equiv N\alpha/3\Lambda$ in Fig. 4.5. The plots show that the spring constant $k_{\mathrm{micro}}(N, \alpha, \Lambda)$ can be scaled by the trade frequency f well.

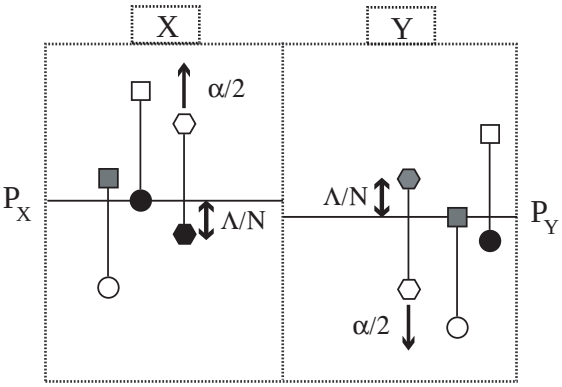

Figure 4.6: A schematic image of the second best bidders' motion. The circles and the squares denote the dealers' bidding price to buy and to sell. The filled circles and the grey squares represent the best bidding prices to buy and sell, respectively. The hexagons denote the second best bidding prices to buy (the filled one) and to sell (the grey one).

In order to determine a reasonable range of the parameters, let us consider the situation in Fig. 4.6, where the arbitrage transaction is about to take place. At the moment, the positions of the second best bidders (hexagons) in the markets X and Y are, on average, Λ/N away from the prices transacted, P_X and P_Y. In the next step, the second best bidders in the markets X and Y will move by $\alpha/2$ on average toward to the prices P_X and P_Y, respectively. The next transaction will be carried out probably by the second best bidders. For $\alpha/2 > \Lambda/N$, the prices of the transactions may move away from each other. The arbitrage transaction cannot bind the two prices of the markets X and Y enough and the two prices P_X and P_Y fluctuate rather freely. It is not a realistic situation. Therefore, the condition

$$f = \frac{N\alpha}{3\Lambda} \leq \frac{2}{3} \tag{4.10}$$

should be satisfied for the real market to be reproduced. On the other side, the simulation data have too large errors in the region $f < 1/3$ because the transaction rarely occurs. We hence use the data in the region $1/3 \leq f \leq 2/3$ hereafter.

The spring constant k_{micro} decays exponentially in the range $1/3 \leq f \leq 2/3$ in both of the plots (a) and (b) of Fig. 4.5, having different slopes. Hence

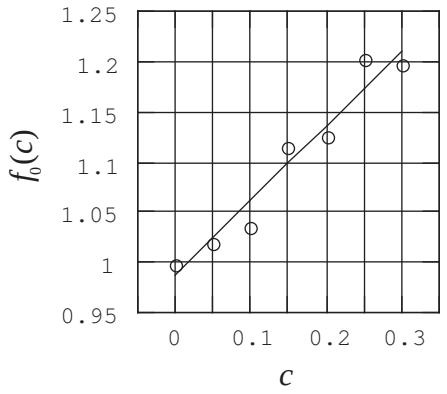

Figure 4.7: The dependence of $f_0(c)$ on c, estimated by fitting the data in Fig. 4.5 as well as the same plots for different values of c.

we assume that the spring constant decays as

$$k_{\text{micro}} \propto e^{-f/f_0(c)}, \tag{4.11}$$

where $f_0(c)$ denotes the characteristic frequency dependent on c. The estimates of the characteristic frequency $f_0(c)$ are shown in Fig. 4.7 as a function of c. The characteristic frequency $f_0(c)$ thus estimated decays linearly with c. The reason why $f_0(c)$ behaves so is an open problem.

In Fig. 4.8, we plot the same data as in Fig. 3.3(b), but by making the horizontal axis the trade frequency f_{real}. In order to compare it with Fig. 4.5 quantitatively, we used the time scale $T_{\text{real}} = 7$[sec]; the interval between two consecutive trades in the actual foreign exchange market is, on average, known to be about 7[sec] [63]. The spring constant in the actual market k is of the same magnitude as k_{micro}. It decays exponentially with the trade frequency f_{real}, which is also consistent with that of the microscopic model shown in Fig. 4.5. The real characteristic frequency in Fig. 4.8, however, is quite different from that of the microscopic model plotted in Fig. 4.5. This is also an open problem.

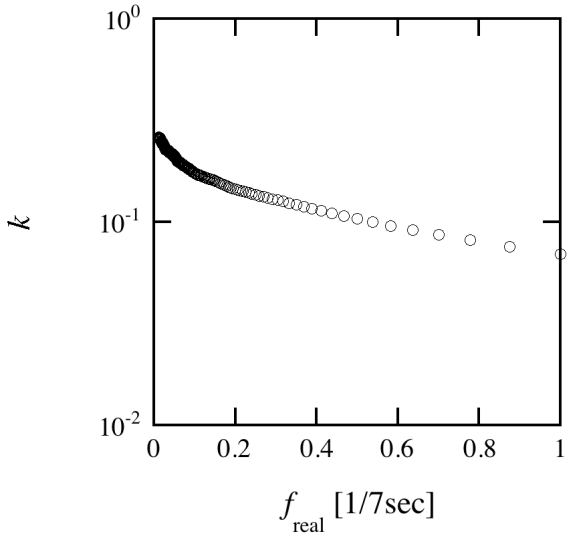

Figure 4.8: We plotted the same data as in Fig. 3.3(b), but the horizontal axis here is the trade frequency scaled by the realistic time scale of the trades, $T_{\text{real}} = 7[\text{sec}]$.

Chapter 5

Summary

In Chap. 2 we showed that triangular arbitrage opportunities exist in the foreign exchange market. The probability density function of the rate product μ has a sharp peak and fat tails. It means that the fluctuations of the exchange rates have correlation that makes the rate product converge to its average $\langle\mu\rangle \simeq 0.99998$. If the rate product μ is greater than unity, the trader can make profit through the above transaction. This is the triangular arbitrage transaction. Once there is a triangular arbitrage opportunity, many traders will make the transaction. This makes μ converge to a value less than unity, thereby eliminating the opportunity. Triangular arbitrage opportunities nevertheless appear, because each rate r_x fluctuates strongly.

In Chap. 3, we first introduced a model including the interaction caused by the triangular arbitrage transaction. We showed that the interaction is the reason of the sharp peak and the fat-tail property of the distribution of the logarithm rate product ν. We also showed that our model is solvable analytically in some cases. Second, on the basis of the model, we showed that the triangular arbitrage makes the auto-correlation function of each rate negative for $n = 1$. The comparison with the actual data is good qualitatively, but it also suggests that the triangular arbitrage of various combinations must be considered. Finally, we explain that the correlation of the foreign exchange rates can appear without actual triangular arbitrage transactions.

In Chap. 4, we introduced the microscopic model, which consists of two systems of the ST model. The microscopic model reproduced the actual behavior of the logarithm rate product ν well. The microscopic model can describe more details than the macroscopic model, in particular, the skewness of the distribution of the logarithm rate product ν. We finally explored the

relation between the spring constant of the macroscopic model and the parameters in the microscopic model. The spring constant of the microscopic model k_{micro} can be scaled by the trade frequency f, and it decays exponentially with f, which is consistent with the spring constant of the actual market k.

Bibliography

[1] H.E. Stanley, L.A.N. Amaral, D. Canning, P. Gopikrishnan, Y. Lee, Y. Liu, Physica A **269** (1999) 156–169.

[2] H.E. Stanley, Physica A **318** (2003) 279–292.

[3] B.B. Mandelbrot, J. Business **36** (1963) 393.

[4] R.N. Mantegna and H.E. Stanley, Nature **376** (1995) 46.

[5] R. N. Mantegna, H. E. Stanley, An Introduction to Econophysics: Cor relations and Complexity if Finance, Cambridge University Press, Cambridge, 1999.

[6] A. Timmermann, Nature **376** (1995) 18.

[7] R.N. Mantegna, Physica A **179** (1991) 232.

[8] P. Gopikrishnan, M. Meyer, L.A.N. Amaral, H.E. Stanley, A.L. Goldberger, Eur. J. Phys. B: Rapid Commun. **3** (1998) 139.

[9] P. Gopikrishnan, V. Plerou, L.A.N. Amaral, M. Meyer, H.E. Stanley, Phys. Rev. E **3** (1998) 139–140 .

[10] X. Gabaix, P. Gopikrishnan, V. Plerou, H.E. Stanley, Physica A **324** (2003) 1–5.

[11] H. Takayasu, M. Takayasu, M.P. Okazaki, K. Marumo, T. Shimizu, in: M.M. Novak (Ed.), Paradigms of Complexity, World Scientific, Singapore, 2000, pp. 243–258.

[12] J.P. Bouchaud, M. Potters, Theory of financial risks, Cambridge University Press, Cambridge, 2000.

[13] J. Voit, The Statistical Mechanics of Financial Markets, Springer, Berlin, 2001.

[14] A. Chatterjee, S. Yarlagadda, B.K. Chakrabarti (Eds.), Econophysics of wealth Distributions, Springer-Verlag, Italia, 2005, and references therein.

[15] V. Pareto, Cours d'Economie Politique, Lausanne, Paris, 1897.

[16] H. Aoyama, W. Souma, Y. Nagahara, M.P. Okazaki, H. Takayasu, M. Takayasu, Fractals **8** (2000) 293–300.

[17] W. souma, Fractals **9** (2000) 463–470.

[18] J.P. Bouchaud, M. Mézard, Physica A **282** (2000) 536–545.

[19] W. Souma, in: H. Takayasu (Ed.) Empirical Science of Financial Fluctuations: The Advent of Econophysics, Springer-Verlag, Tokyo, pp. 343–352.

[20] Y. Fujiwara, W. Souma, H. Aoyama, T. Kaizoji, M. Aoki, Physica A **321** (2003) 598–604.

[21] K. Okuyama. M. Takayasu, H. Takayasu, Physica A **269** (1999) 125–131.

[22] M.H.R. Stanley, L.A.N. Amaral, S.V. Buldyrev, S. Halvin, H. Leschhorn, P. Maass, M.A. Salinger, H.E. Stanley, Nature **379** (1996) 621.

[23] L.A.N. Amaral, S.V. Buldyrev, S. Havlin, H. Leschhorn, P. Maass, M.A. Salinger, H.E. Stanley, M.H.R. Stanley, J. Phys. I France **7** (1997) 621.

[24] Y. Lee, L.A.N. Amaral, D. Canning, M. Meyer, H.E. Stanley, Phys. Rev. Lett **81** (1998) 3275.

[25] H. Takayasu, K. Okuyama, Fractals **6** (1998) 67.

[26] S.V. Buldyrev, L.A.N. Amaral, S. Havlin, H. Leschhorn, P. Maass, M.A. Salinger, H.E. Stanley, M.H.R. Stanley, J. Phys. I France **7** (1997) 621.

[27] H. Takayasu, H. Miura, T. Hirabayashi, K. Hamada, Physica A **184** (1992) 127.

[28] T. Hirabayashi, H. Takayasu, H. Miura, K. Hamada, Fractal **1** (1993) 29.

[29] A.-H. Sato, H. Takayasu, Physica A **250** (1998) 231–252.

[30] D. Chowdhury and D. Stauffer, A generalized spin model of financial markets, Eur. Phys. J. B **8** (1999) 477–482.

[31] R. Cont, J.P. Bouchaud, Macroeconomic Dynamics **4** (2000) 170–196.

[32] K. Sznajd-Weron, R. Weron, Int. J. Mod. Phys. C **13** (2002) 115–123.

[33] J.C. Hull, Options, Futures, and Other Derivatives, Prentice-Hall (1989).

[34] J.C. Hull, Introduction to Futures and Options Markets, Prentice-Hall (1991).

[35] B. B. Mandelbrot, J. Business **36** (1963) 394–419.

[36] E.-F. Fama, J. Finance **25** (1970) 383.

[37] Z. Ding, C. W. J. Granger, R. F. Engle, J. Emprical Finance **1** (1993) 83.

[38] M.M. Dacorogna, U.A. Muller, R.J. Nagler, R.B. Olsen, O.V. Pictet, J. Int. Money Finance **12** (1993) 413.

[39] Y. Liu, P. Cizeau, M. Meyer, C.-K. Peng, H. E. Stanley, Physica A **245** (1997) 437–440.

[40] R.N. Mantegna, Eur. Phy. J. B., **11** (1999) 193–197.

[41] V. Plerou, P. Gopikrishnan, B. Rosenow, L.A.N. Amaral, H.E. Stanley, Phys. Rev. Lett, **83** (1999) 1471–1474.

[42] V. Plerou, P. Gopikrishnan, B. Rosenow, L. A. N. Amaral, H. E. Stanley, Physica A **287** (2000) 374–382.

[43] L. Kullmann, J. Kertesz, R.N. Mantegna, Physica A **287** (2000) 412–419.

[44] B.B. Mandelbrot, Quant. Fin., **1** (2001) 123–130.

[45] L. Kullman, J. Kertesz, K. Kaski, Phys. Rev. E, **66** (2002) 026125.

[46] J.-P. Onnela, A. Chakraborti, K. Kaski, Phys. Rev. E, **68** (2003) 056110.

[47] T. Mizuno, S. Kurihara, M. Takayasu, H. Takayasu, in: H. Takayasu (Ed.) The Application of Econophysics, Proceedings of the Second Nikkei Symposium, Springer-Verlag Tokyo, 2004, pp.24–29.

[48] H. Tastan, Physica A **360** (2006) 445–458.

[49] B. Toth, J. Kertesz, Physica A **360** (2006) 505–515.

[50] W.-S. Jung, S. Chae, J.-S. Yang, H.-T. Moon, Physica A **361** (2006) 263–271.

[51] I. Moosa, Quantitative Finance **1** (2001) 387–390.

[52] Y. Aiba, N. Hatano, H. Takayasu, K. Marumo and T. Shimizu, Triangular arbitrage as an interaction among foreign exchange rates, Physica A **3**10 (2002) 467–479.

[53] M. Mavirides, Triangular arbitrage in the foreign exchange market: inefficiencies, technology, and investment opportunities, Quorum Books, 1992.

[54] R. N. Mantegna, H. E. Stanley, An Introduction to Econophysics: Correlations and Complexity in Finance, Cambridge University Press, Cambridge (1999) pp.64–67.

[55] R. F. Engle, Econometrica **50** (1982) 987–1002.

[56] T. Bollerslev, J. Econometrics **31** (1986) 307–327.

[57] Y. Aiba, N. Hatano, H. Takayasu, K. Marumo, T. Shimizu, Physica A **324** (2003) 253–257.

[58] Y. Aiba, N. Hatano, H. Takayasu, K. Marumo, T. Shimizu, in: H. Takayasu (Ed.) The Application of Econophysics, Proceedings of the Second Nikkei Symposium, Springer-Verlag Tokyo, 2004, pp.18–23.

[59] J. P. Bouchaud, M. Potters, Theory of Financial Risks: From Statistical Physics to Risk Management, Cambridge University Press, Cambridge (2000) p.34 and pp.56–63.

[60] H. Takayasu, M. Takayasu, M. P. Okazaki, K. Marumo and T. Shimizu in *Fractal Properties in Economics,* Paradigms of Complexity, World Scientific, ed. Miroslav M. Novak, (2000) pp.243–258

[61] R. N. Mantegna, Phys. Rev. E **4**9 (1994) 4677–4683.

[62] Y. Aiba, N. Hatano, Physica A **344** (2004) 174–177.

[63] T. Ohira, N. Sazuka, K. Marumo, T. Shimizu, M. Takayasu, H. Takayasu, Physica A **308** (2002) 368–374.